

THE UNIVERSITY OF HONG KONG
DEPARTMENT OF PHYSICS

PHYS2533 DIRECTED STUDIES IN PHYSICS
PROJECT REPORT

The night sky brightness in Hong Kong

Project supervisor: Dr. J.C.S. Pun

Author: TSANG Tsz Ho

University Number: 2006309343

Abstract

The aim of this project is to study the night sky brightness in Hong Kong. 1283 sets of night sky brightness data were taken by the Sky Quality Meter (SQM) at 18 districts of Hong Kong for the 'survey of light pollution in Hong Kong'. They were analyzed to study the relation with the moon and the air pollutants' concentration. The relation with the moon was tested against Krisciunas' past studies, considerable agreement was found. The air pollutants were analyzed individually and there was no concrete relation found. The night sky brightness at the Space Museum and the Sai Kung iObservatory was found to differ by 4 magnitudes per square arcsecond on average at midnight. The feasibility of using all-sky camera's image to determine the night sky brightness was also studied. The maximum difference with the SQM reading was found to be about 2 magnitudes per square arcsecond.

Content

1. Introduction.....	5
2. Apparatus and methodology.....	7
2.1 A Survey of light pollution in Hong Kong.....	7
2.1.1 SQM specifications.....	7
2.1.2 Selection of observing sites and time.....	8
2.1.3 Data format, collection and processing.....	9
2.2 SQM-LE system.....	9
2.2.1 SQM-LE specifications.....	9
2.2.2 Setup of system.....	9
2.2.2.1 Power over Ethernet.....	10
2.2.2.2 SQM-LE Casing.....	10
2.2.2.3 SQM Reader.....	11
2.2.3 Data collection and processing.....	13
2.3 Moon phase and position calculation.....	14
2.3.1 Motivation.....	14
2.3.2 Calculation Algorithm.....	14
2.3.3 Results verification.....	15
2.3.4 Use in the light pollution survey.....	16
2.4 Moonlight's effect calculation.....	16
2.4.1 Theory.....	16
2.4.2 Predicted results.....	17
2.4.3 Use in light pollution survey.....	19
2.5 Air quality correlations with NSB.....	19
2.6 All-sky camera.....	20
2.6.1 Apparatus.....	20
2.6.1.1 Fisheye lens.....	20
2.6.1.2 Imaging device.....	21
2.6.2 Observation	21
2.6.3 Image reduction.....	22

2.6.4 Sky brightness estimation.....	22
3. Results.....	24
3.1 Light pollution survey.....	24
3.1.1 Moon phase effect on sky brightness.....	24
3.1.2 Theoretical prediction of sky brightness.....	25
3.1.3 Air pollution's effect on sky brightness.....	28
3.2 SQM-LE system data analysis.....	30
3.2.1 Macroscopic trends.....	30
3.2.2 NSB Comparison for two sites.....	32
3.2.3 Time consistence of NSB.....	34
3.2.4 Abnormal peaks and discontinuities.....	37
3.3 All-sky camera data analysis.....	38
3.3.1 Targeted field.....	38
3.3.2 Plate scale estimation.....	38
3.3.3 Sky brightness estimation.....	40
4. Sources of error and improvements.....	44
4.1 Reliability of SQM readings.....	44
4.2 Casing of SQM-LE.....	44
4.3 All-sky camera images.....	44
5. Acknowledgement.....	45
6. Appendix	
6.1 C++ program script for the moon phase/ position calculation.....	46
6.2 C++ program script for the change in magnitude calculation.....	55
7. Reference.....	57

1. Introduction

The invention of incandescent light bulbs in 1879 by Thomas Edison¹ has undoubtedly been marked as one of the major roles on the stage of technological advancement. Throughout years and years of improvement, lighting is now not limited to using light bulb. Fluorescent lamp and light emitting diode (LED) are now coming to replace conventional light bulbs by their greater output power and efficiency.

However, outdoor lighting has been inducing a problem of improper use. Street light, advertisement boards, decoration light are present around any cities on the world offering safety, commercial development and brilliant night view. Those are beneficial to mankind when used properly. Excess amount and improperly directed light is what light pollution is all about. A great deal of energy is wasted, together with the disappearance of stars on the brightened night sky. The brightening of night environment can in fact turn the biological clocks and calendar of wild species into wrong steps² and be related to lots of human health problems such as depression and cancer³.

Many projects have been conducted to raise people's awareness on the current situation of light pollution. The 'Earth hour' project has invited millions of world citizen to switch off the unnecessary light from 20:30 to 21:30 on 28th March 2009. To target the age group of children and the young, social groups on Facebook⁴ and My Space⁵ are developed to spread the information of light pollution and the negative side effects it brings.

On the theoretical side, a preliminary model to predict the natural night scene has been developed by Jensen⁶ by taking into account the light from the moon, the stars, the zodiacal light and the atmosphere. The model was tested by creating a picture simulating the night scene at the Little Matterhorn. Such theoretical model simulates the effect of natural light sources as viewed on the earth surface.

On the practical side the brightness distributions over the entire piece of night sky were measured by Duriscoe⁷ et al by dividing the panoramic sky images taken from a wide-field CCD into small segments for individual photometric measurements using reference stars in the raw data frames. It was done in more than 80 different locations throughout US for a detailed study of the night sky conditions and the effect of artificial light, as an effort to protect such beautiful natural resource. The Johnson

V band magnitude of the reference stars, which is a reasonable approximation of human eye's perception of sky brightness, was chosen for the calibration of data frames. Together with the atmospheric extinction coefficients determined for each data set, all-sky panoramic brightness representations, darkest, brightest and integrated sky brightness magnitudes were obtained to show the effect of light pollution and light pollution controls. Most of the sites produce darkest sample points of about 22 MPSAS, a benchmark for an unpolluted sky; while the brightest 15.62 MPSAS at the Government Wash suggests considerable light pollution.

On the other hand, the properties of the sky at Calar Alto observatory were studied between 2004 and 2007⁸. The first dark time night-sky spectrum (taken on moonless nights between dusk and dawn) containing the light pollution emission lines was studied. It reveals the contribution of the mercury lines to the sky brightness in the B, V and R band are about 0.09, 0.16 and 0.16 MPSAS respectively. The zenith night sky brightness values were measured in the U, B, V, R, I band to be about the 22 MPSAS benchmark except for I band. A higher extinction coefficient due to increase in aerosol extinction and a better seeing condition were found in the summer season. This analysis may later suggest the possibility of building new optical telescope at the Calar Alto observatory.

In order to study how the night sky brightness in Hong Kong varies temporally and geographically, the data collected from the 'A Survey of Light Pollution in Hong Kong' and from a preliminary computer based SQM system was studied. The feasibility of using an all-sky camera to estimate the sky brightness was also investigated in this project.

The report starts with the discussion of the apparatus and the methods used in the project including the specifications of apparatus, data formats, calculation algorithms and the processing of raw data. The results and the analysis is then summarized in section 3 followed by the sources of error and improvements in section 4.

2. Apparatus and methodology

2.1 A Survey of light pollution in Hong Kong

The University of Hong Kong was funded by the “Environment and Conservation Fund” in 2007 to conduct a survey on the light pollution in Hong Kong. In the course of the survey, participants are invited to use the handy device provided by the University, Sky Quality Meter (SQM) discussed in next section, to measure the night sky brightness (NSB) near where they live. The data collected by about two hundreds of participants over two hundreds of sites are gathered on the web¹⁰ to study the time and place variations of sky brightness, and the dependence on various factors.

2.1.1 SQM specifications^{11,12}

The Sky Quality Meter (SQM) is a portable device, Figure 1, developed by Unihedron to measure the NSB in the unit of magnitude per square arcsecond (MPSAS), which is equivalent to the same magnitude’s starlight spread over a square sky field of view of size one arcsecond by one arcsecond. The detector in the SQM is a light intensity to frequency converter, and the SQM convert the output frequency to a digital LED reading. The sensor is covered by a near-infrared blocking filter. This filter is introduced to guarantee the brightness reading is contributed mainly by the targeted visible light. The absolute precision of the meter is $\pm 10\%$ or $\pm 0.10\text{MPSAS}$. It is sensitive to light from a cone of Half Width Half Maximum (HWHM) of about 42 degrees, which is the angle at which the central brightness falls by half.

A similar device SQM-Lens is also adopted in the survey, the major difference is the additional lens in front of the detector to narrow down the field of view to 10 degrees HWHM and thus data are subject to less variation near the horizon, Figure 2.



Figure 1. Sky Quality Meter



Figure 2. Sky Quality Meter Lens

2.1.2 Selection of observing sites and time

To figure out the light pollution situation all over Hong Kong, students and campsites helpers among 18 Hong Kong districts were invited to participate in the project which is divided into four phases, individual durations are shown in Table 1.

Phase	Duration (DD-MM-YYYY)
1	15-03-2008 to 31-05-2008
2	28-06-2008 to 30-09-2008
3	01-10-2008 to 31-12-2008
4	07-02-2009 to 31-05-2009

Table 1. Duration of the four phases in the survey¹⁰

The sites covered are shown in the map below, Figure 1.

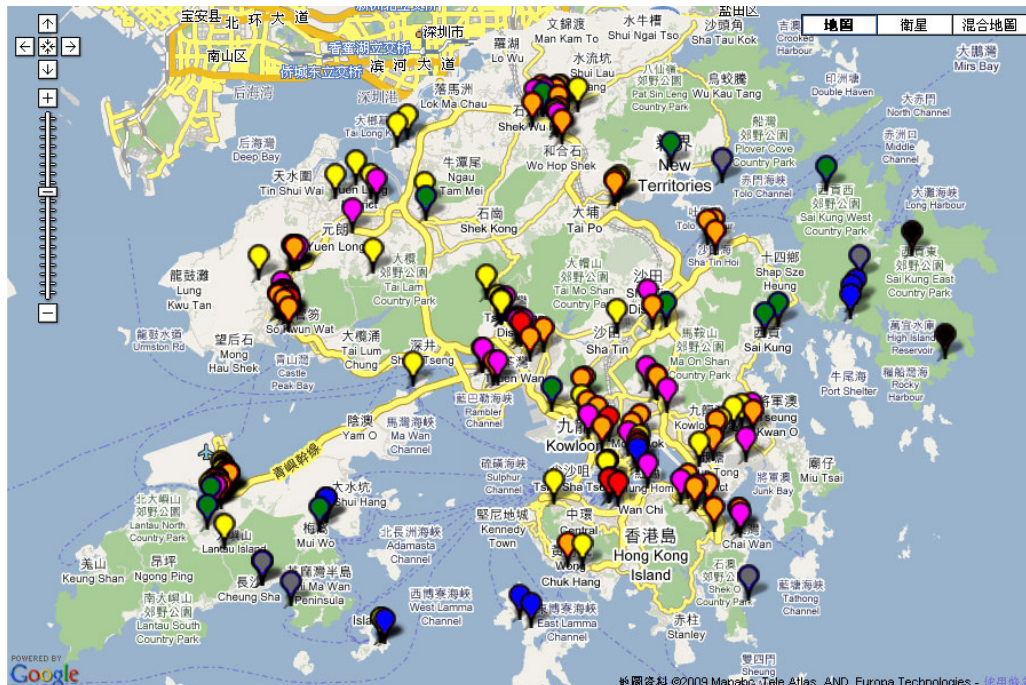


Figure 3. Observing sites on the survey¹⁰

Observing sites selection

In selecting any of the observing sites, participants were advised to adopt sites that are least affected by artificial light and has a wide field of view. Photographs taking each compass direction on each site, the longitude and latitude values from Google Earth¹³ were also required to report to the web database.

Observing time selection

Trying to eliminate as much as variation induced by participants' choice of observation date and time, regular observing time slots were assigned, they are 21:30 and 23:30 on 5th, 10th, 15th, 20th, 25th and possibly 30th in every month. Data collected from these times can also be used to study the effect of human activities since less artificial light is expected at the later time.

2.1.3 Data format, collection and processing

In each set of observation data, five NSB values are obtained by pointing the SQMs as near to the zenith as possible, together with one temperature value. Naked-eye grading of cloud and haze density are also recorded in scales of 1-5 and 1-3 respectively with 5 and 3 indicating no clouds or haze for each data set. All the above mentioned data sets are stored in Microsoft Access format with the corresponding observation date and time. The data are then uploaded by the participants to the survey web page. The detailed procedure of reporting observation sites and uploading data are shown in the survey web page.

2.2 SQM-LE system

2.2.1 SQM-LE specifications¹¹

Sky Quality Meter Lens Ethernet (SQM-LE) is the Ethernet enabled version of SQM-Lens for which data can be taken upon computer command rather than human hands. The actual working principle and specifications of SQM-LE are similar to that of the SQM and the SQM-Lens, with 10 degrees HWHM and the same data precision.

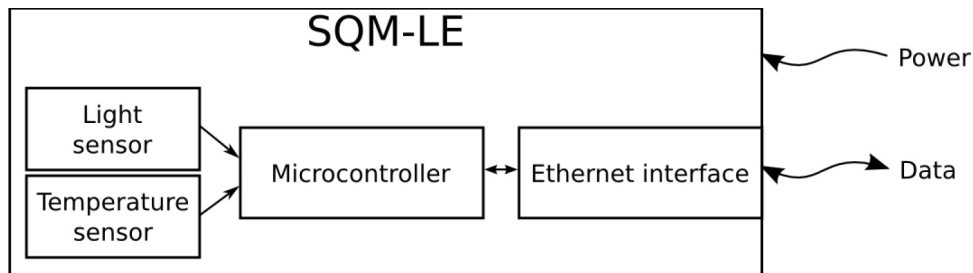


Figure 4. Schematic diagram of SQM-LE¹⁴

2.2.2 Setup of system

In the survey discussed in section 2.1, the focus is on the geometrical variations of NSB among different districts in Hong Kong. Due to the need of manpower, only few data sets can be obtained in each night on each observing site. With the development of SQM-LE, automatic NSB monitoring systems can now be set up to

study the time variation and compare the trends on specific sites. As a preliminary test, two sites: Space Museum (in urban Tsim Sha Tsui) and the iObservatory (in suburban Lady MacLehose Holiday Village) were selected. The data obtained could then be used to compare the NSB in terms of human population density.

2.2.2.1 Power over Ethernet

To record the NSB, the SQM-LE must be mounted outdoor with power supply and network connections, where immediate availability is absent. The method adopted to setup outdoor power supply and network connection was by means of a plug-and-play device called Power over Ethernet (PoE), D-Link DWL-P200. Basically it combines the power and network transmission into one single Category 5 Ethernet cable, the middle green cable in Figure 5. The devices below the green cable in the Figure were placed outdoor.

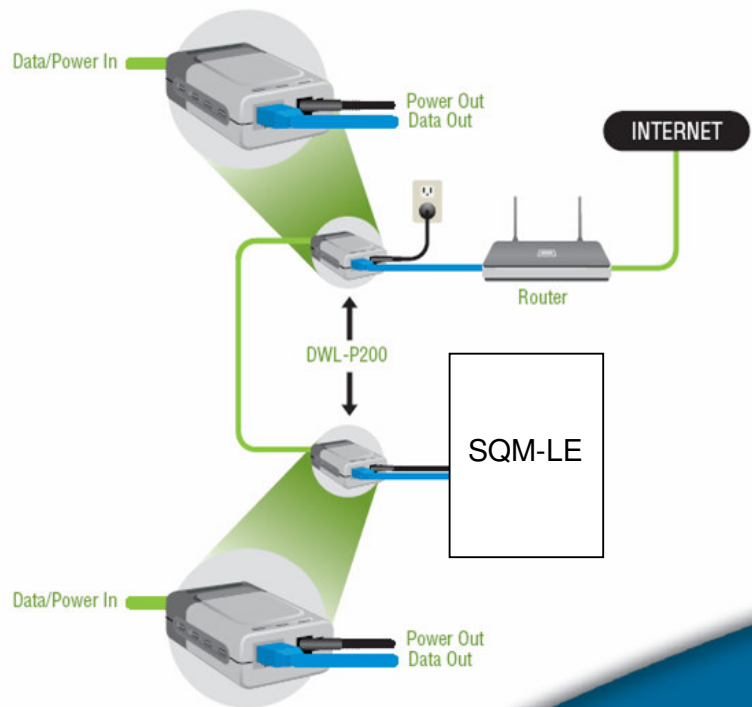


Figure 5. The schematic diagram of SQM-LE setup with PoE¹⁵

2.2.2.2 SQM-LE Casing

The outdoor components of the system should be protected from the environmental impacts to maintain its stability and reliability. A plastic case with black inner shielding was chosen in this early setup, Figure 6. The black shielding was intended to block the unwanted side light which may contribute error to the NSB values, especially in the urban Space Museum. A clear window without shielding was left opened on the casing top for proper NSB measurement, Figure 7.



Figure 6. The plastic casing



Figure 7. The top window opened for the SQM-LE

2.2.2.3 SQM Reader

The free software SQM Reader developed by the Knightware¹⁶ was used to monitor both SQM-LEs. It works by recognizing the assigned fixed IP address of the SQM-LE to issue a data-taking command upon clicking the 'Read Now' button. The NSB value in MPSAS will then displayed instantaneously on the software interface, Figure 8. Alternately, a regular command can be issued by setting the frequency under the 'Minutes' entry and press the 'Read Every' button. Adding a tick in the 'Save readings to' box would automatically save the readings taken in a Comma Separated Values (CSV) plain text file (.txt) containing all the data shown in Figure 8, with every reading occupying a single line.

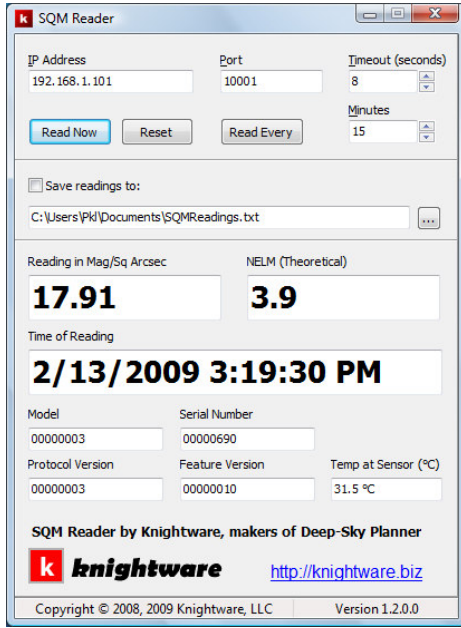


Figure 8. An example SQM Reader interface

The entry named NELM means the Naked Eye Limiting Magnitude. It is the theoretical estimated magnitude of the dimmest star appeared to naked eye. The formulae¹⁷ relating MPSAS and NELM in magnitude are

$$NELM = 7.93 - 5 \times \log_{10}(10^{4.316 - (NSB/5)} + 1) \quad (1)$$

$$MPSAS = 21.58 - 5 \log(10^{(1.586 - NELM / 5)} - 1) \quad (2)$$

This gives the SQM Reader's value when correct to 1 decimal place. A plot of the NELM against the MPSAS in Figure 9 shows the almost linear correspondence in between.

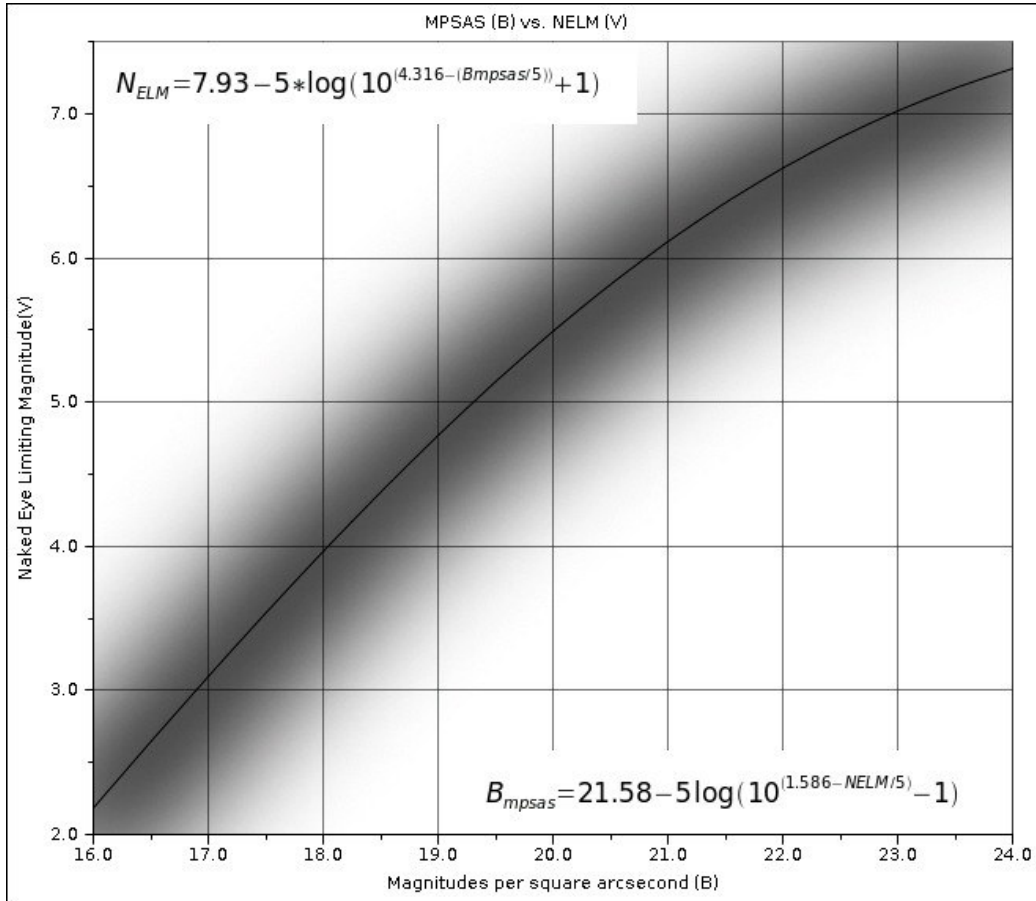


Figure 9. NELM and MPSAS relation¹¹

2.2.3 Data collection and processing

The NSB values were taken every five minutes on both sites and the output text files were collected. They were all first combined into one single Excel file by applying the ‘Test to Columns’ entry under the ‘Data’ menu.

The Space Museum computer was using Chinese Windows so the CSV files from there contain Chinese characters indicating am/pm. It has brought difficulties in plotting the NSB data as the Excel is incapable of recognizing that.

Such problem was solved by using the DATE(year, month, day) and the TIME(hour, minute, second) functions in the Excel library. First separate the time and date into six separate columns and then equate the seventh column with the sum of the two functions. Right-click on the resultant column and set the ‘Cell Format’ as desired.

It was observed that the reading intervals were not identically five minutes on both sites. Those delays may be due to tiny network speed and system fluctuations. Extra care should be taken when more SQM-LEs are set up in a network.

2.3 Moon phase and position calculation

2.3.1 Motivation

Apart from the artificial light, natural light sources contributing to the NSB also call for astronomers concerns. The major natural sources are the moon, the sun, the planets and stars, zodiac light, airglow and diffuse galactic and cosmic light⁶. The sun's role here is not the daily direct sunlight but the astronomical twilight coming out from the edge of horizon near sunrise and sunset. As we are now investigating the sky brightness at night, the major contributor is the moon.

Throughout the nights, the moon moves across the sky at different time, position and with various phases. Light is collected from a cone rather than a point on sky in all kinds of the SQMs' measurement. The presence and the status of the moon should contribute to some degree in the NSB readings taken. To study whether and how the moon and the NSB correlates, the moon's position and phase on a particular date and time is calculated.

A C++ computer program was then constructed to compute the values for the moon.

2.3.2 Calculation Algorithm

The moon, the earth and the sun are mutually perturbing one another in their orbits so we cannot ignore the sun and go straight to the moon-earth system computation. The sun's position is the first value needed to go any further.

For easy visualization and computational convenience, the geocentric model is adapted to assume it is the sun that moves around the earth in elliptical orbit. The typical time scale used in astronomical calculation is the Day number (the number of days as decimal number) from a commonly agreed moment of time, an epoch. The epoch chosen here is J2000, that is, 1st January 2000 at 12:00:00 UT. The position of the sun at any instant can then be calculated from the orbital elements (essential values to fully describe the orbit) of the sun's apparent orbit around the earth.

The rough position of the moon can be found similarly by the orbital elements of the moon and the calculated position of the sun. Perturbations are then applied to the rough value to improve the accuracy to within 1 to 2 arcminutes¹⁹, such precision is enough for the application here as the moon's size is already accounting for half a degree, or equivalently 30 arcminutes.

The orbital elements and thus the results obtained are all in ecliptic coordinates.

Transformations to the equatorial and then to the horizontal coordinates are performed to get the final position of the moon as seen in Hong Kong.

The phase of the moon is then calculated from the relative position of the moon and the sun as seen on the earth, assuming they are moving on the same plane. The

formula finding the phase F is $F = \frac{1}{2}(1 - \cos D)$ (3)

D is denoted in Figure 10. The value $F=1$ corresponds to full moon whereas $F=0$ corresponds to new moon.

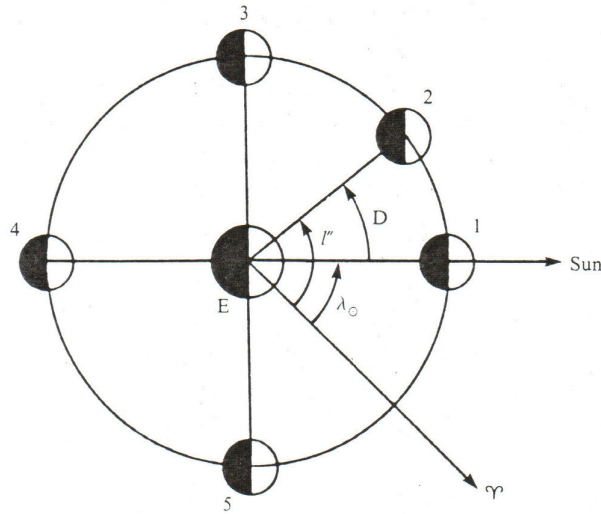


Figure 10. Finding the phase of the moon

2.3.3 Results verification

The constructed C++ program was tested against reliable sources to pinpoint any algorithmic and coordinate transformation error.

The calculated position of the moon is tested by comparing with the values predicted by the Hong Kong Observatory (HKO)²⁰ for the mid-autumn festivals in 2009, 2010 and 2011, results are tabulated in Table 2.

Date (DD-MM-YYYY)	Time (HH:MM)	Altitude (Degree)		Phase
		HKO	C++ program	
02-10-2009	22:56	67	67.52	0.972
03-10-2009	23:38	73	73.20	0.996
05-10-2009	00:23	79	78.77	0.998
21-09-2010	22:59	63	63.65	0.972
22-09-2010	23:39	68	68.72	0.995

24-09-2010	00:20	74	73.77	0.999
11-09-2011	23:42	64	64.58	0.995
13-09-2011	00:24	69	69.43	0.999
14-09-2011	01:05	74	74.15	0.984

Table 2. Comparison between HKO prediction and the program calculated values

From the last three columns, it is observed that the altitude agrees quite well and the phase is very close to 1 as known for mid-autumn festivals. Therefore, the program was believed to be reliable and used for the NSB analysis with the data gathered in the light pollution survey.

2.3.4 Use in the light pollution survey

Over one thousand date-time values of the survey database were input to the C++ program and azimuth, altitude and phase values of the moon were calculated. They were tabulated in an Excel file together with the corresponding NSB, cloud and haze indexes.

2.4 Moonlight's effect calculation

2.4.1 Theory

The mathematical calculation of the effect of moonlight on the NSB was based on Kriscuinas's paper named 'A model of the brightness of moonlight' dated 1991²¹. The brightness of the sky is correlated with the phase and the angular separation

Atmospheric scattering plays the major role on the brightening effect brought by the presence of the moon. The effect is based on a model by dividing the field of view cone into discs of infinitesimal thickness. The atmospheric scattering effect contributed by each of the disc is estimated and integrated to obtain the net effect of magnitude. Here only the moon is modeled so the sky background is assumed to be constant across the night sky.

Using the above model suggested by Kriscuinas, the change in brightness dV of a particular sky position is calculated from a given moon phase and angular separation with the moon. The following formulae are extracted and modified from Kriscuinas' paper²¹.

$$\text{Illuminance of the moon } \log_{10} I = -0.4(3.84 + 0.026|d| + 4 \times 10^{-9} d^4) \quad (4)$$

where $d = 180^\circ - D$ and D is given in Figure 10.

$$\text{Scattering function } f(\rho) = 10^{5.36} [1.06 + \cos^2(\rho)] + 10^{6.15 - \rho/40} \quad (5)$$

ρ is the angular distance between the sky position and the moon on a great circle joining them, which is equal to 90 minus the altitude here.

$$\text{Scattering airmass } \chi(Z) = (1 - 0.96 \sin^2 Z)^{-0.5} \quad (6)$$

Z is the zenith distance in degree for the moon or the sky. With our assumption $Z=0$ for the sky and $Z=\rho$ for the moon.

The following two formulae express the brightness value B in the other brightness unit nano-Lamberts (nL), which is related to MPSAS by equation (7).

$$nL = 34.08 \exp(20.7233 - 0.92104 \text{MPSAS}) \quad (7)$$

$$\text{Dark nighttime sky brightness } B_0(Z) = B_{zen} 10^{-0.4k(\chi-1)} \chi \quad (8)$$

B_{zen} is the mean dark sky brightness value equals 21.59 MPSAS.

$$\text{Model surface brightness of the moon } B_{moon} = f(\rho) I \cdot 10^{-0.4k\chi(\rho)} [1 - 10^{-0.4k\chi(Z)}] \quad (9)$$

k is the extinction coefficient of value 0.172.

Finally, with equations (4) to (9) the change in sky brightness in MPSAS is given by equation (10) below.

$$\Delta V = -2.5 \log[(B_{moon} + B_0(Z)) / B_0(Z)] \quad (10)$$

Value of ΔV is then computed for each data set of the light pollution survey to study the theory predicted effect.

2.4.2 Predicted results

Since the SQMs all collect light from a cone of more than ten degrees of HWHM, the present situation thus differs from the theory in which a point on sky has to be specified for the calculation. In the application of the above theory, therefore, one assumption has been made. The observed sky positions were assumed to be at the zenith, which is justifiable by noting the angular response of the SQM used in the light pollution survey. That was obtained by Cinzano¹² and is shown in Figure 10.

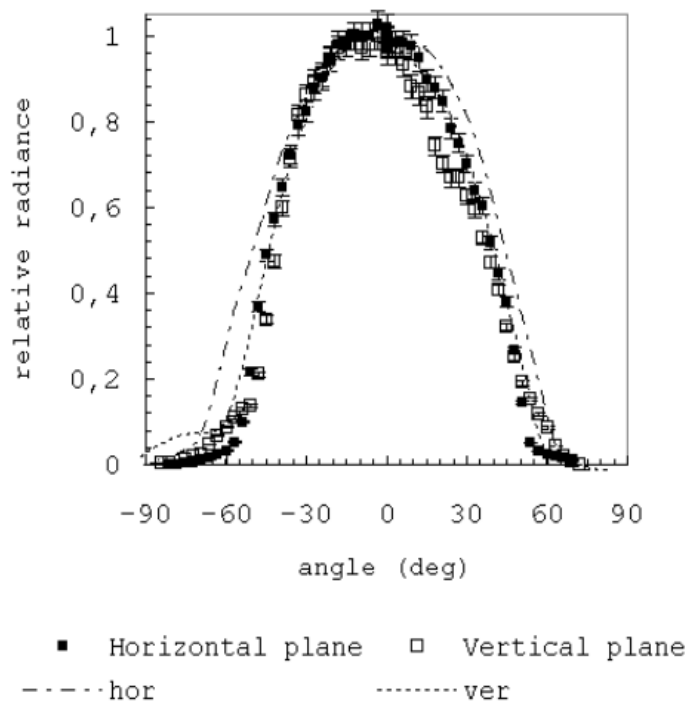


Figure 11. Response curve of the SQM (relative radiance versus angle)¹²

Based on the assumption made, the changes in NSB magnitude (dV) were calculated and plotted. Figure 12 shows the plot of dV against the moon phase by placing the moon at different altitude

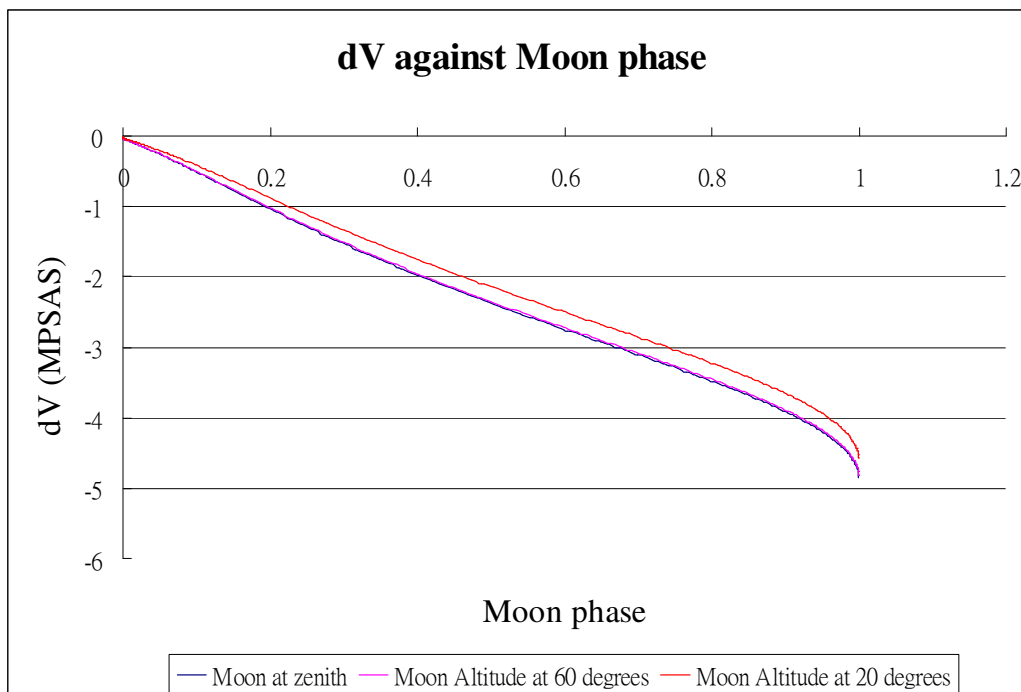


Figure 12. Change in magnitude against moon phase

This reveals the predicted NSB difference due to a full moon could be about -4.5 MPSAS, which is equivalent to more than 60 times brighter. The dV trends with increasing moon phase is nearly linear beside an observable dip when attaining full moon. A shift of the moon by 30 degrees down from zenith to 60 degrees altitude causes only tiny change in sky brightness as seen from the corresponding overlapping curves.

Alternately, change in magnitude dV is plotted in Figure 13 against the altitude by adjusting the moon phase. At each altitude, dV tends to saturate at about 50 degrees and any up shifting of the moon induces slight change in sky brightness.

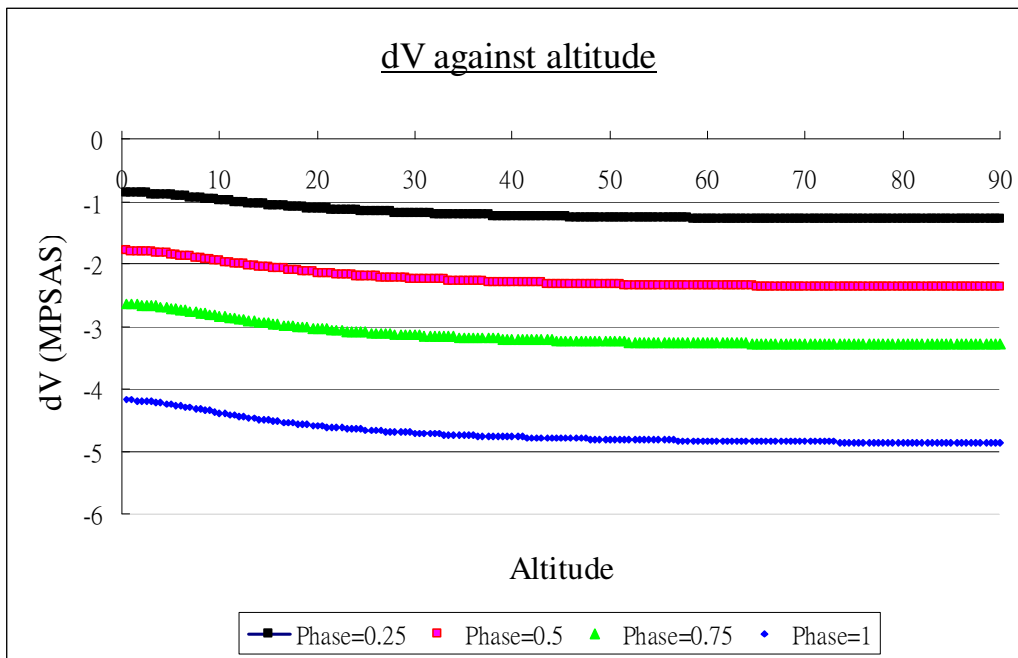


Figure 13. Change in magnitude against altitude

2.4.3 Use in light pollution survey

Using the program discussed in section 2.3, the moon phase was calculated for each date and time of the survey database. The moon-sky separation was estimated by formula $(90 - \text{altitude})$ with the assumption explained in 2.4.2. Theoretical predictions of the moon's effect in terms of the change in NSB value in MPSAS were calculated for each of the corresponding date and time.

2.5 Air quality correlations with NSB

Apart from the apparent moon's brightening of the night sky, two kinds of air quality data were downloaded from the Environmental Department's website²². One is

the Air Quality Data (AQD) measured hourly by 11 general stations and 3 roadside stations over Hong Kong, another is the Air Pollution Index (API) measured in the same 14 stations. AQD includes concentration of five air pollutants including Sulphur Dioxide (SO_2), Respirable Suspended Particles (RSP), Nitrogen Oxides (NO_x), Nitrogen dioxide (NO_2) and Carbon Monoxide (CO). All the concentrations are in micrograms per cubic meter ($\mu\text{g}/\text{m}^3$) except CO which is in $10\mu\text{g}/\text{m}^3$.

Both the AQD and API are taken at the start of every hour. The data at 21:00 and 23:00 were chosen to represent the state of air pollution with the NSB values gathered by the light pollution survey at 21:30 and 23:30 respectively. The AQD data was updated until 31st September, 2009 so that only the data from phase 1 and 2 can be used, while the API online is nearly real time.

The NSB values were plotted against the corresponding air quality data to study whether there is any observable relation.

2.6 All-sky camera

To study the feasibility in using photometric method to analyze the NSB from CCD images, all-sky camera capable of taking a large piece of sky was chosen and the specifications of the equipment are listed in the following section.

2.6.1 Apparatus

2.6.1.1 Fisheye lens

The Nikon AF Fisheye 16mm f/2.8D fisheye lens was adopted for its wide angle of view so that the image frames could be filled up with as much useful information of the sky as possible. The 'D' following f/2.8 suggests the presence of hand adjusted aperture ring.

The official specifications of the lens are listed below²³.

Lens construction: 8 elements in 5 groups

Full-frame (135) field of view: 180 degrees (diagonal)

Dimensions: 63×57mm

Aperture diameter: 600mm

The actual horizontal field of view of the lens is not the diagonal 180 degrees, but a narrower 137 degrees²⁴.

2.6.1.2 Imaging device

The CCD camera used in this analysis is the Santa Barbara Instruments Group (SBIG) STL-11000M. Model of the CCD chip is KAI-11000M interline CCD. Some specifications are listed below²⁵.

Array: 4008×2672 pixels

Pixel size: 9 microns square

Peak quantum efficiency (QE): 50% at 500nm

Image area: 36mm×24.7mm

Full well capacity: 50,000 e^-

Gain: 0.840 e^- /ADU

The actual wavelength dependence of quantum efficiency is shown in Figure 14 for reference.

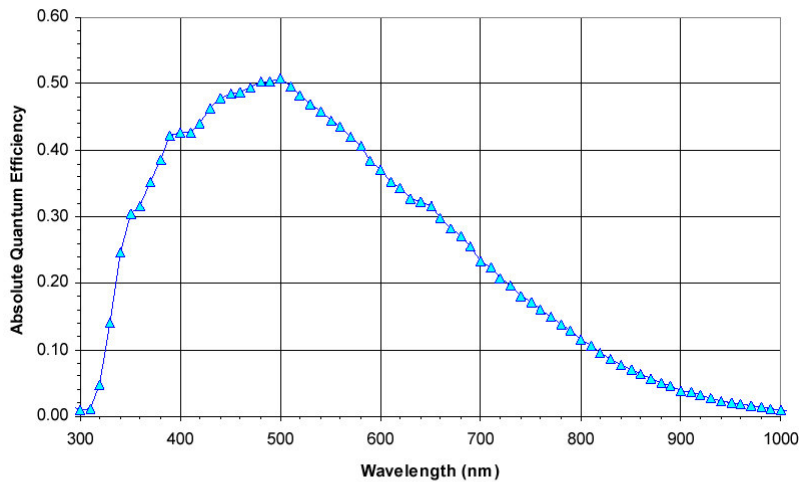


Figure 14. Quantum efficiency of KAI-11000M interline CCD chip²⁶

2.6.2 Observation

The observation was made after the midnight of 17th March 2009 at about 02:00 to 03:00 at the iObservatory in Sai Kung with no filter mounted on the lens. The moon was above the horizon when the images were taken so that it contributed to some extent of brightening.

Images of two exposure times were taken, one for 30 seconds and one for 60 seconds. Both frames were taken with 1×1 binning mode.

Four dark frames were taken for each exposure. Bias and flat frame were not taken as the bias frame is already included in the dark frame and it was difficult to obtain an

evenly laminated surface for the flat frame.

2.6.3 Image reduction

Image reduction was carried out by using common astronomical software named Image Reduction and Analysis Facility (IRAF)²⁷. The images are all in Flexible Image Transport System (FIT) format which can be displayed and manipulated using the viewer named SAOImage DS9²⁸. Suitable brightness and contrast level were adjusted by right-clicking the mouse and dragging up and down in the DS9 interface.

A master dark frame was created by median stacking the four using the IRAF task ‘imcombine’. There are three combining schemes available in this task, namely average, median and sum. The median was chosen and others parameters were left as default. All the IRAF parameters can be viewed and modified using the commands ‘lpar task’ and ‘epar task’ respectively.

The master dark frames corresponding to two exposure times were then subtracted from the raw data frames using the IRAF task ‘imarith’ with the operator ‘-’. The resultant data frames were then ready for the sky brightness analysis.

2.6.4 Sky brightness estimation

The NSB is estimated by the method of relative photometry. In astronomy, the magnitude of a celestial object is calculated by the formula

$$m = -2.5 \log(\text{flux}) + c \quad (11)$$

where c is a constant depends on the filter chosen. In the present application, no filter was used in all the data frames.

Such formula is the definition so it applies both to stars and the sky background. Subtracting the formula for the sky by that of a reference star,

$$m_{sky} = m_{star} - 2.5 \log(\text{flux}_{sky} / \text{flux}_{star}) \quad (12)$$

The flux of any reference star is estimated by the IRAF task ‘imexamine’²⁹. Enter ‘imexamine’ and the mouse will become a blinking round cursor on the display. Place the cursor above the brighter stars in the data frames on which flux are to be estimated. Press the key command ‘a’ and the estimated x-y coordinates, flux estimated by circular aperture photometry f_{out} , peak count around the cursor will then be displayed as a text output. The value f_{out} is not the actual flux from the stars and the actual flux is related to the output value by

$$flux_{star} = \frac{f_{out} \times Gain}{QE} \quad (13)^{30}$$

For the sky background, uniform patches without stars were chosen for the IRAF task ‘imexamine’ with key command ‘m’. This task display the statistical results of mean, median, standard deviation, minimum and maximum counts for a 5×5 pixels box as a text output. The median output counts $f_{out,sky}$ were taken as the values used for the flux calculation using the same equation (13). The sky flux so obtained is in a single pixel representing a particular portion on the sky. The size of such portion depends on the optics and imaging devices used so the value does not carry much scientific meaning. Therefore, the sky flux calculated from the equation (13) should be further divided by the angular field of view per pixel in the unit of square arcsecond. As a result, the actual sky flux is calculated from

$$flux_{sky} = \frac{f_{out,sky} \times Gain}{QE} \cdot \frac{1}{FOV} \quad (14)^{30}$$

The angular field of view FOV in MPSAS is calculated by

$$FOV = P_H \cdot P_V \quad (15)^{30}$$

where P_H and P_V are the plate scales in the horizontal and vertical direction respectively.

Since a fisheye lens was used for all the data frames, it is expected that the plate scale across the image does not stay as constant. The plate scales at different parts of the image were estimated by dividing the angular distance between two known reference stars by their distance in pixels. The angle between two stars on the celestial sphere was computed by their Right Ascension (RA) and Declination (Dec) found in the online database of the Set of Identifications, Measurements, and Bibliography for Astronomical Data (SIMBAD)³¹ using the java program online³². The distance in pixels was calculated by the x-y coordinates of reference stars obtained on the DS9 displaying interface.

With the above information, the sky brightness in MPSAS can then be computed by equation (12) with the star magnitude m_{star} found in the SIMBAD database.

3. Results

3.1 Light pollution survey

3.1.1 Moon phase effect on sky brightness

In studying the moon's brightening effect, it is preferable to have as many data points and to eliminate any uncertainty of night sky conditions. Therefore, two campsites joined since phase 1 of the survey were selected for NSB analysis with the moon's effect. Namely, they are the Po Leung Kuk Jockey Club Tai Tong Holiday Camp in Yeun Long (Location A) and the Salvation Army Bradbury Camp in Cheung Chau (Location B). To focus on the moon's effect, the dates with the moon about the horizon were used in the database.

Figure 15 and 16 shows the relation between the average NSB from the 5 readings and the calculated moon phase with error bars showing the standard error of the SQM readings.

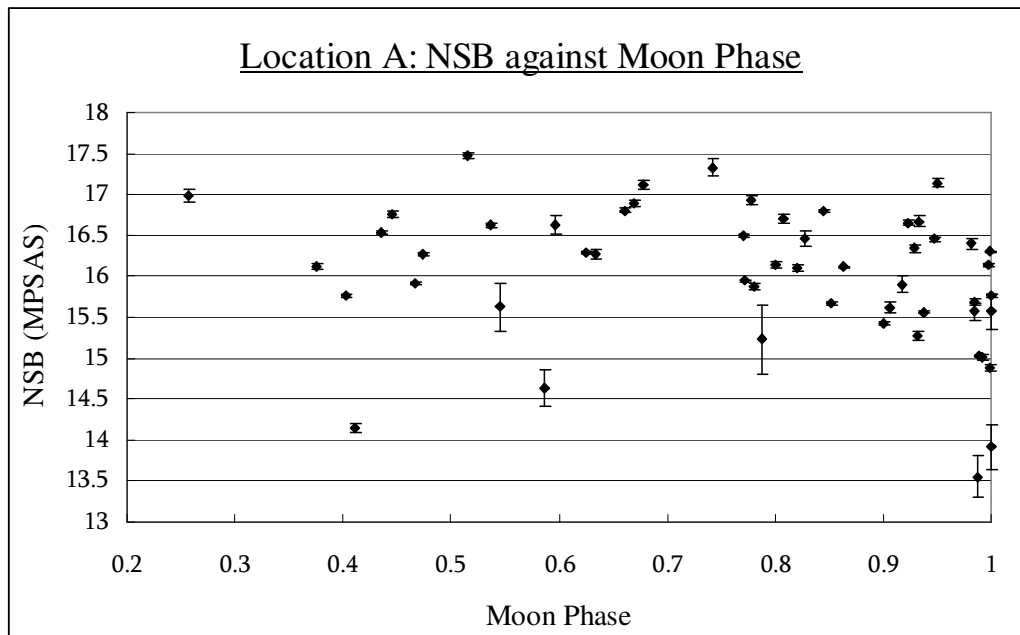


Figure 15. NSB against moon phase for Location A (Yeun Long)

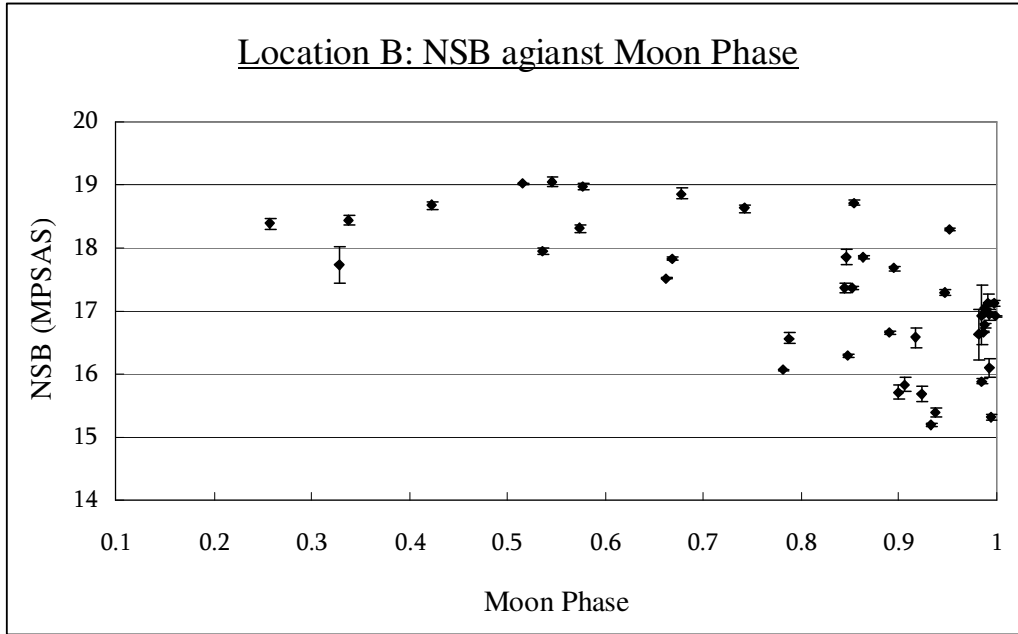


Figure 16. NSB against moon phase for Location B (Cheung Chau)

From the plots, several observations are noticed and interpreted.

In both plots, the NSB value drops (sky become brighter) with increasing moon phase which is expected. Even though they are both campsites in suburban area of Hong Kong, the maximum sky magnitude can differ by 1.5 MPSAS or equivalently by 4 times. Ignoring the data points with relatively larger error, the dipping trend of NSB near full moon in Figure 12 is reproduced here in both locations.

However, such a trend should not be attributed completely to the effect of the moon phase's variation. From the data reported the cloud indexes assessed by different observers range from 1 to 5 whereas the haze indexes range from 1 to 3. The presence of such perturbations in the atmospheric conditions should also be taken into consideration when interpreting the graphs.

3.1.2 Theoretical prediction of sky brightness

From the model suggested by Kriscuinas, the change in sky magnitude dV in both locations for the dates plotted in 3.1.1 was calculated. Since the theory predicts only the change in magnitude, a sky background should be added so that the theory prediction can be compared with the SQM values on the same graphs. The sky background brightness is set as the maximum mean sky brightness on the dates which are to be plotted. Here it is assumed that the maximum SQM value corresponds to the darkest possible environment contributed solely by the sky without clouds and haze. Figure 17 and 18 compare the actual SQM readings with the theory prediction.

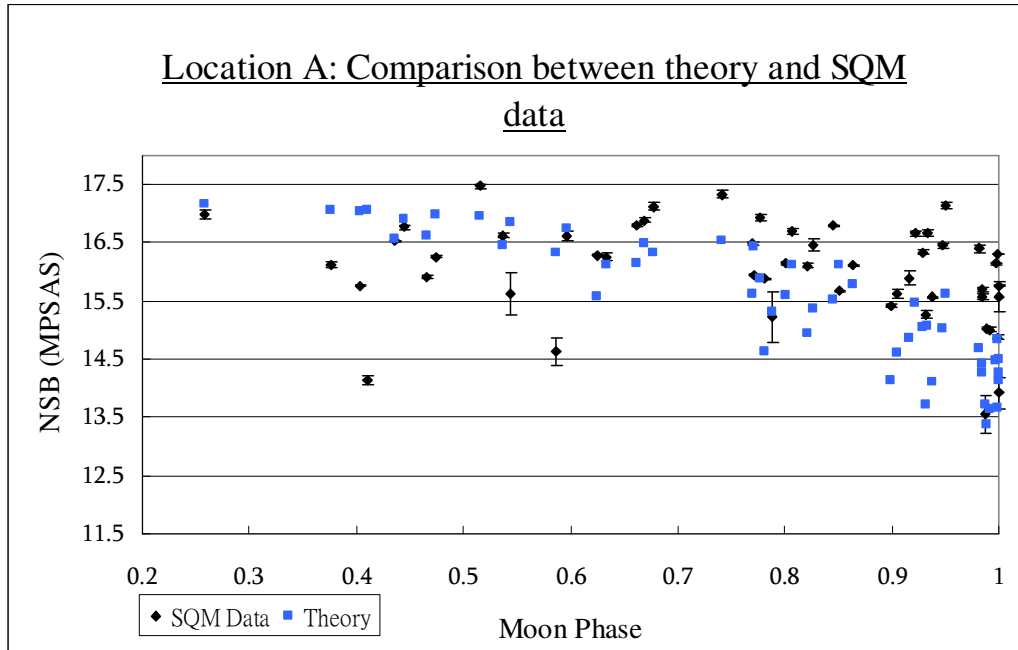


Figure 17. NSB comparison with theory for Location A (Yuen Long)

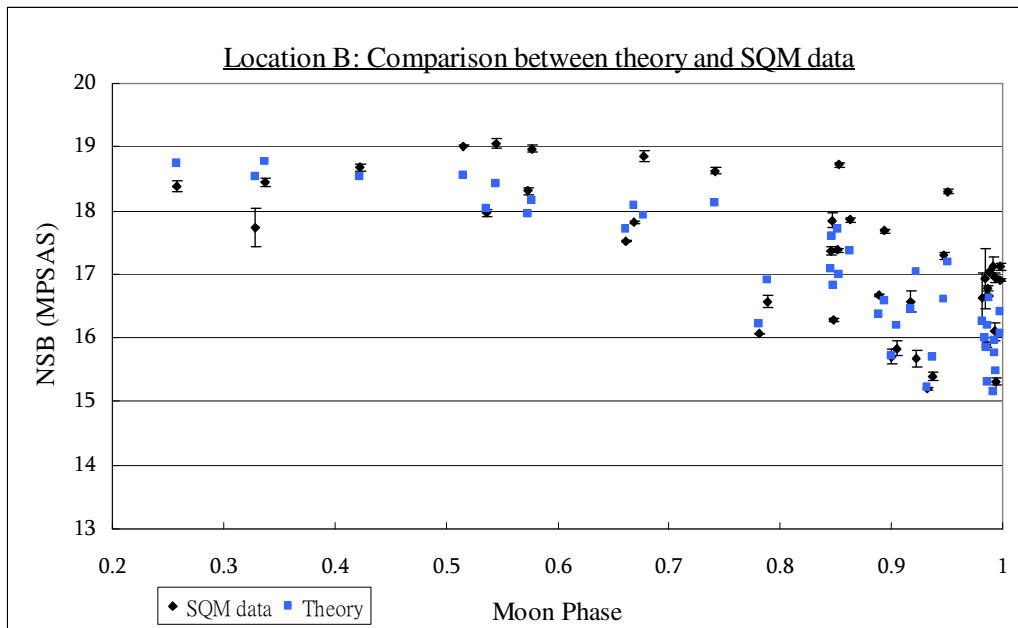


Figure 18. NSB comparison with theory for Location B (Cheung Chau)

To assess the accuracy of the prediction, the SQM data in Figure 17 and 18 is subtracted from the corresponding prediction value and plotted again with moon phase. By definition, a positive difference means the predicted sky is darker than reality and vice versa. Similarly, error bars are representing the standard error of the data obtained with SQMs.

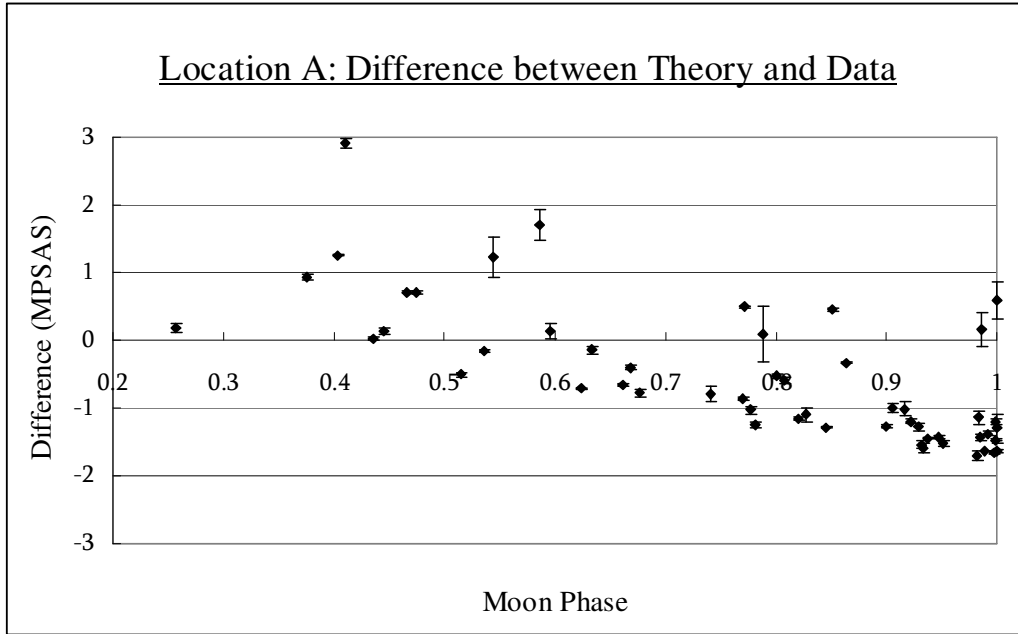


Figure 19. Comparison between moonlight theory and SQM data for Location A

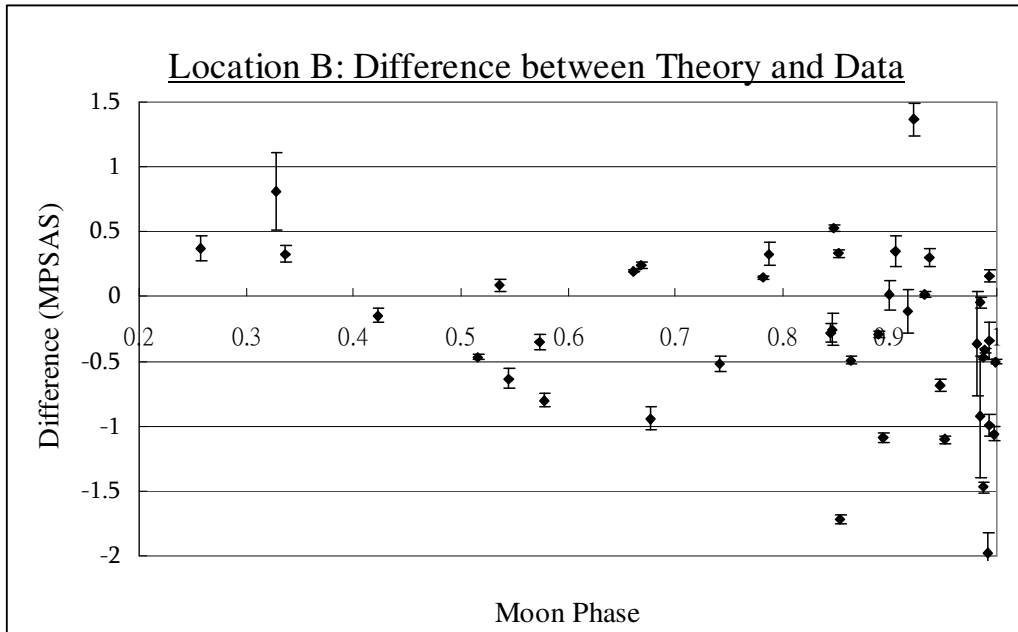


Figure 20. Comparison between moonlight theory and SQM data for Location B

As in Figure 19 and 20, the change in sky magnitude brought by the moon was predicted to be up to -4 MPSAS that is a brightening by nearly 40 times. The predicted NSB is always smaller than the observation values for moon phase greater than 0.5, as implied by the negative difference. This may be explained by the light pollution problem because the brightening role of the moon will be of less importance

in an originally brighter background.

On the contrary, the prediction gives a darker sky than reality when the moon phase is smaller than 0.5, as implied by the positive difference. It is also understandable as the theory takes into account only the moon but not any other factors. The presence of artificial light, clouds and haze may also contribute to the real sky brightness which is not accounted for in the theory.

	Location A		Location B	
Absolute value of difference	Number of datapoint	Percentage %	Number of data points	Percentage %
<3	53/53	100	43/43	100
<2	52/53	98.11	43/43	100
<1.5	44/53	83.02	41/43	95.35
<1	24/53	45.28	36/43	83.72
<0.9	23/53	43.40	33/43	76.74
<0.8	22/53	41.51	31/43	72.09
<0.7	17/53	32.08	31/43	72.09
<0.5	12/53	22.64	26/43	60.47
<0.4	9/53	16.98	22/43	51.16
<0.3	8/53	15.09	13/43	30.23
<0.2	8/53	15.09	8/43	18.60
<0.1	2/53	3.77	4/43	9.30

Table 3. Analysis of accuracy of prediction

In both locations, the difference is within 2 MPSAS except for one data point in Location A. Table 3 shows that the prediction at Location B is better as more than half of the absolute difference is less than 0.4 MPSAS. However, no conclusion can be made for the moon phase dependence of the magnitude difference between prediction and data as there is no concrete trend observed.

3.1.3 Air pollution's effect on sky brightness

To investigate air pollutants' effect on the sky brightness, the NSB values from the survey were plotted against the concentrations and the API value. Here only Location A in Yuen Long was investigated, Location B was left out due to its lack of data points during phase 1 and 2.

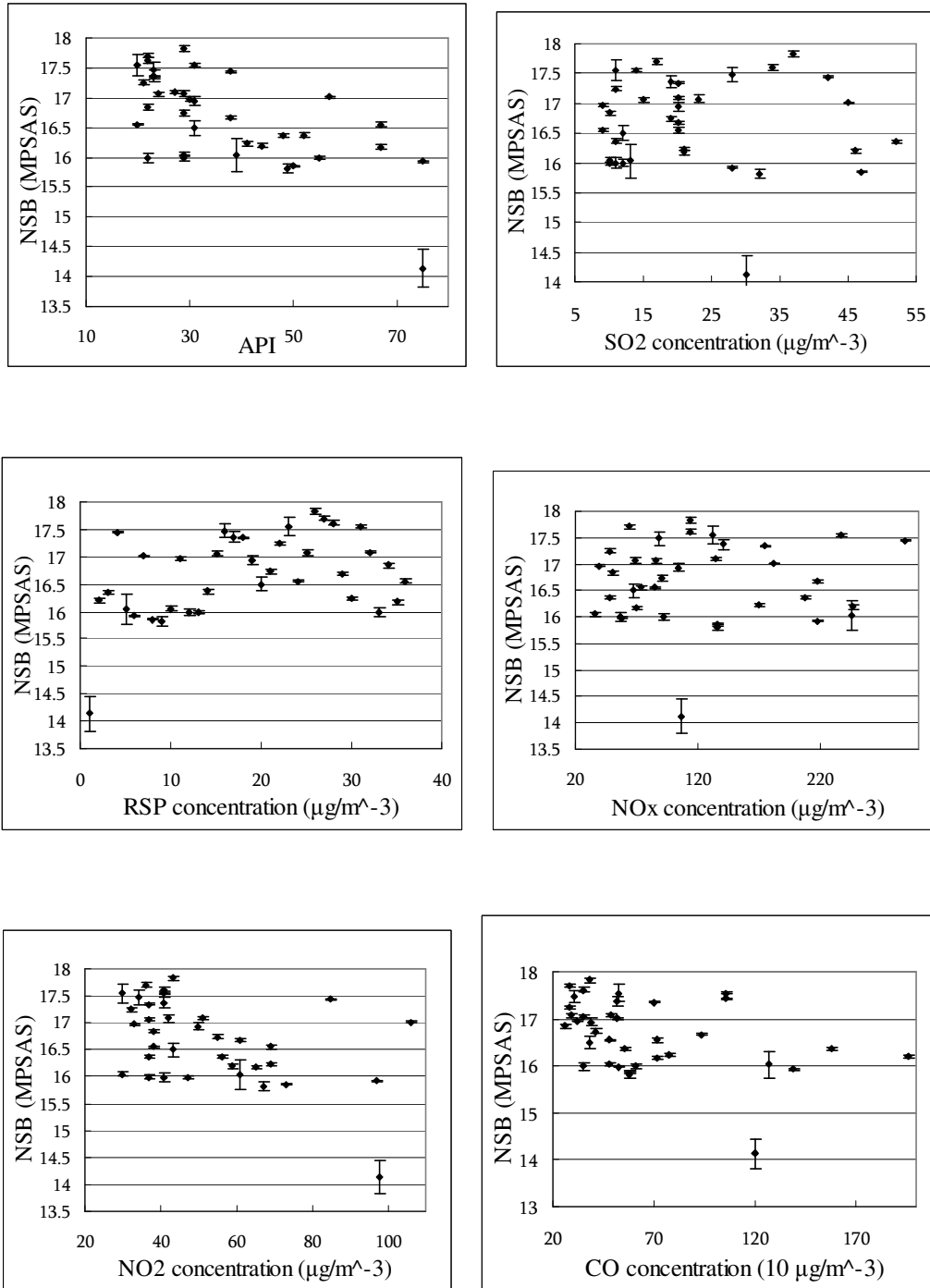


Figure 21 to 26. NSB in MPSAS against pollutants' concentration in $\mu\text{g}/\text{m}^3$

From the above plots, no observable trend can be observed. This may be due to the chaotic atmospheric conditions that cannot be revealed by such simple relations. In fact, the difference in concentrations between 21:00 and 23:00 two hours apart can

be as large as $89\mu\text{g}/\text{m}^3$ for nitrogen oxide. It suggests the one-hour time interval between air quality measurements and two NSB measurements per night may be not enough that the relation could not be resolved. The limitation of the SQM reading taking frequency is exactly what the SQM-LE system aim to resolve.

3.2 SQM-LE system data analysis

3.2.1 Macroscopic trends

The SQM-LE system provides a platform of continuous monitoring of the sky brightness which is previously limited by the need of manpower in the light pollution survey. The preliminary systems on both observing sites were set up on 2nd March 2009 and allowed to operate independently. The data obtained from 2nd March 2009 to 10th March 2009 are plotted against time to study the macroscopic trends.

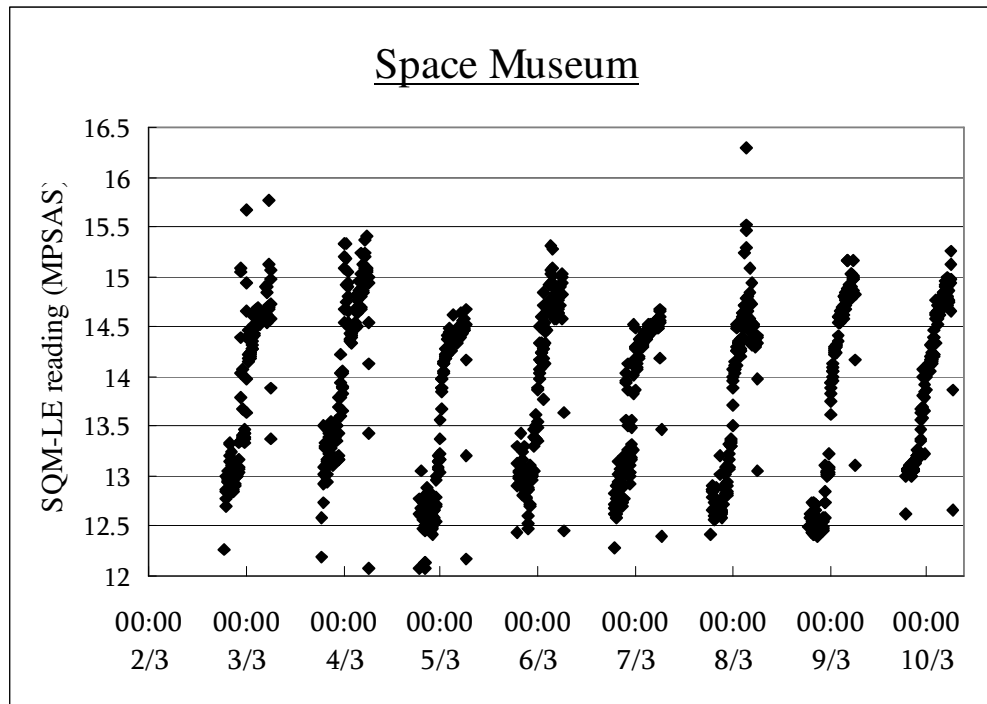


Figure 27. Macroscopic trends in Space Museum. Vertical axis is NSB in MPSAS and the horizontal axis is the date and time.

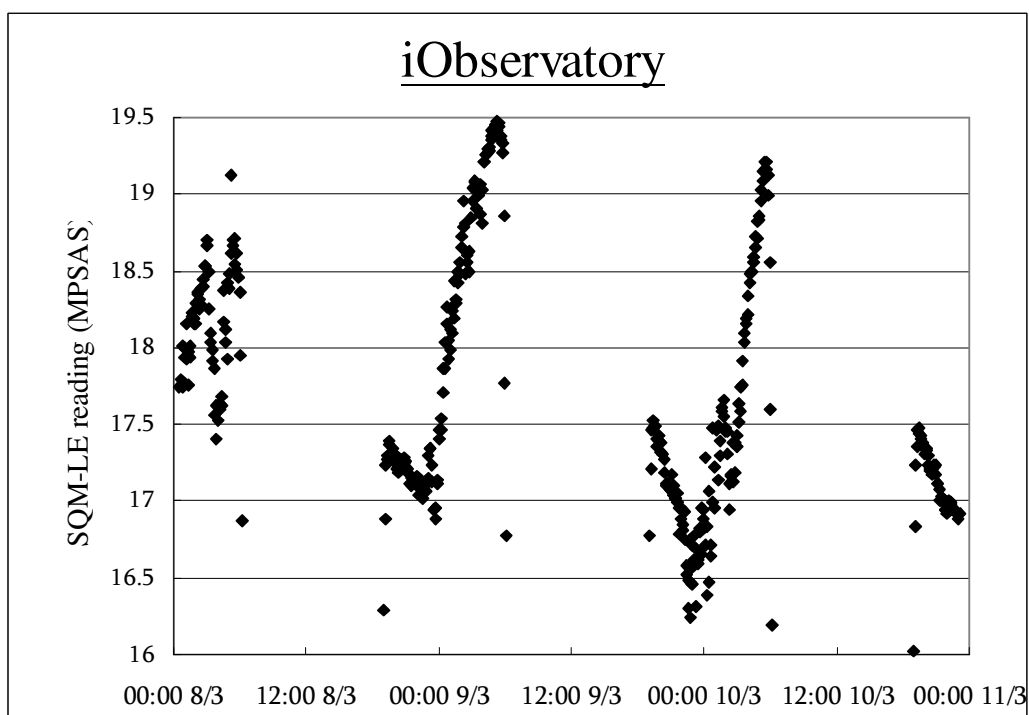
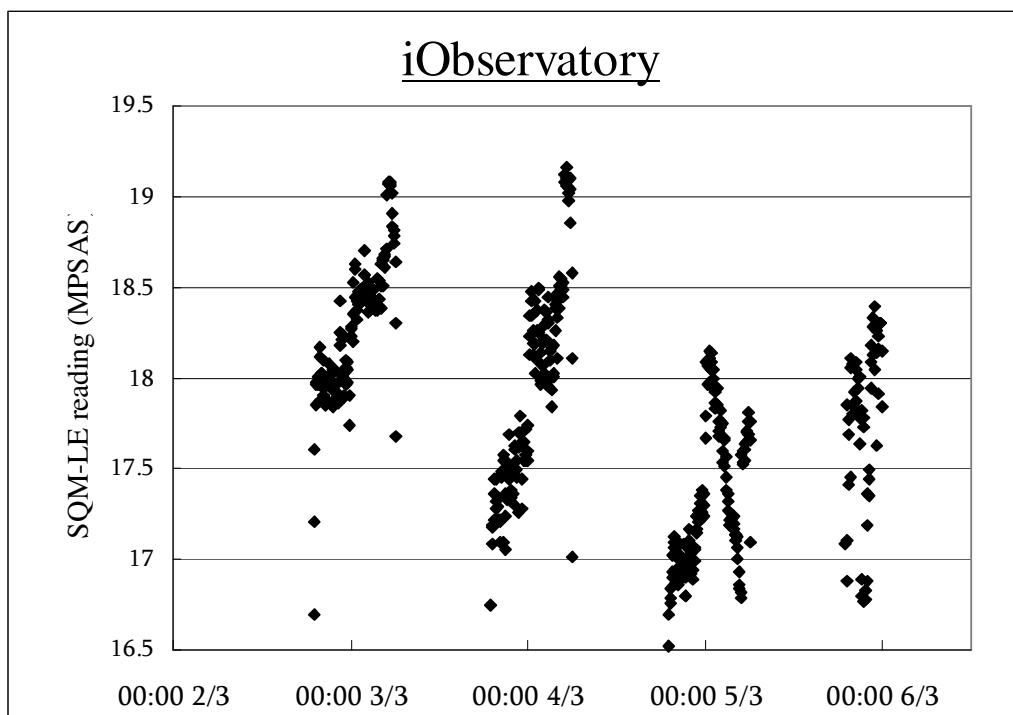


Figure 28 and 29. Macroscopic trend in iObservatory.

The splitting of plot at iObservatory is due to the temporary loss of data due to the electric power suspension in a heavy rain. The NSB generally obeys an increasing trend across the night due to the decrease in human activities. As in the Space Museum, there are consistent jump in NSB at midnight. This may be due to some regular turning off of light at midnight. At the iObsevatory, the trend is generally continuous with some turbulence caused by the heavy rain.

3.2.2 NSB Comparison for two sites

For comparison, the differences in SQM-LE reading at two nights are plotted in Figure 30 and 31. They are selected because of the smoother trends and the other nights are influenced by raining. The positive values for the difference suggest that the night sky is constantly dimmer at the rural area Sai Kung. Both plots suggest that the difference in NSB decreases at later night. This may be due to the saturation of NSB upon reduction of human activities so the NSB is contributed mainly by natural conditions.

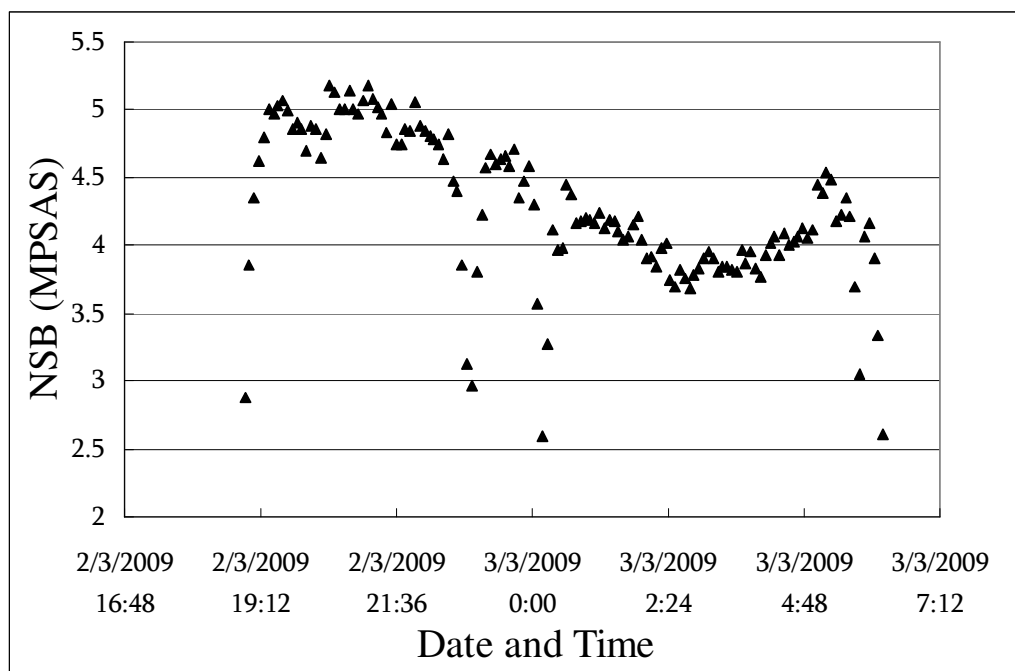


Figure 30. NSB difference between two sites. Positive for higher value in iObs.

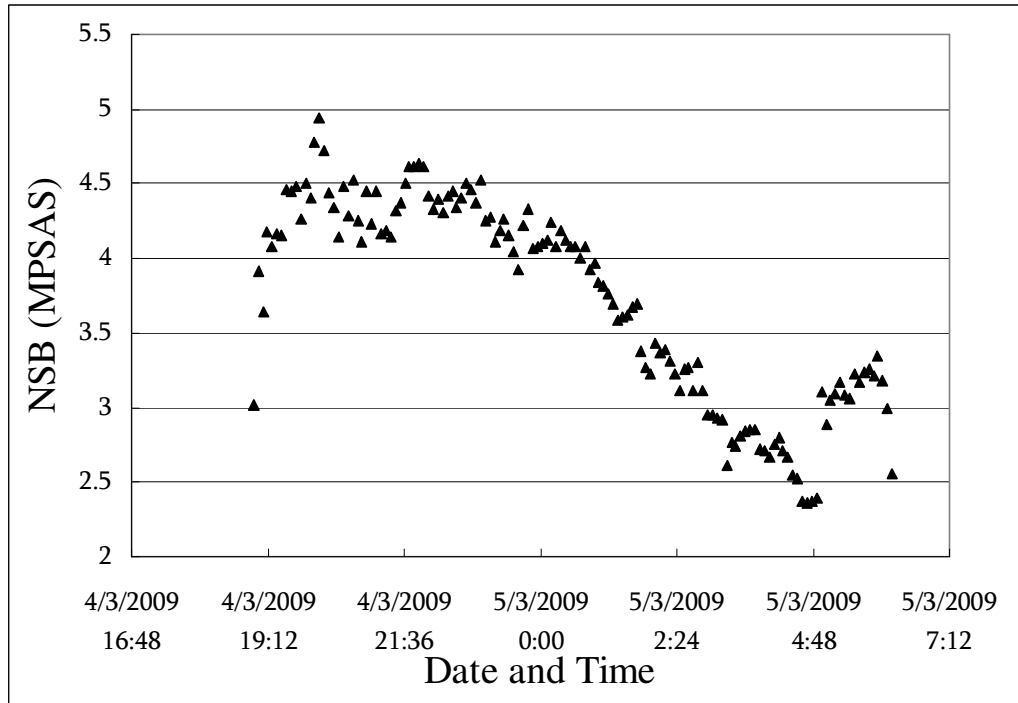


Figure 31. NSB difference between two sites. Positive for higher value in iObs.

	Figure 30	Figure 31
21:00-22:00	4.955	4.403
22:00-23:00	4.360	4.413
23:00-00:00	4.490	4.160
00:00-01:00	3.932	4.082
01:00-02:00	4.142	3.598
02:00-03:00	3.831	3.238
03:00-04:00	3.876	2.808
04:00-05:00	4.016	2.606

Table 4. Average differences between NSB at both sites, at one-hour intervals.

The 02:00-03:00 interval records the minimum value of difference at Figure 30's time. In Figure 31, it records a constantly decreasing trend in the difference after 22:00. This trend is not observed for the time of Figure 30, the major cause may be the two spikes near midnight which will be discussed in the next section.

It is observed that the sky magnitude can differ by up to 4.9 MPSAS that is equivalent to 91 times of difference.

3.2.3 Time consistence of NSB

To verify the time consistence of NSB, the NSB for the two periods of time is plotted. One is before midnight, the other is after midnight. Due to the temporary loss of electrical power, one three days' data can be plotted for the iObservatory site whereas five days are available for Space Museum.

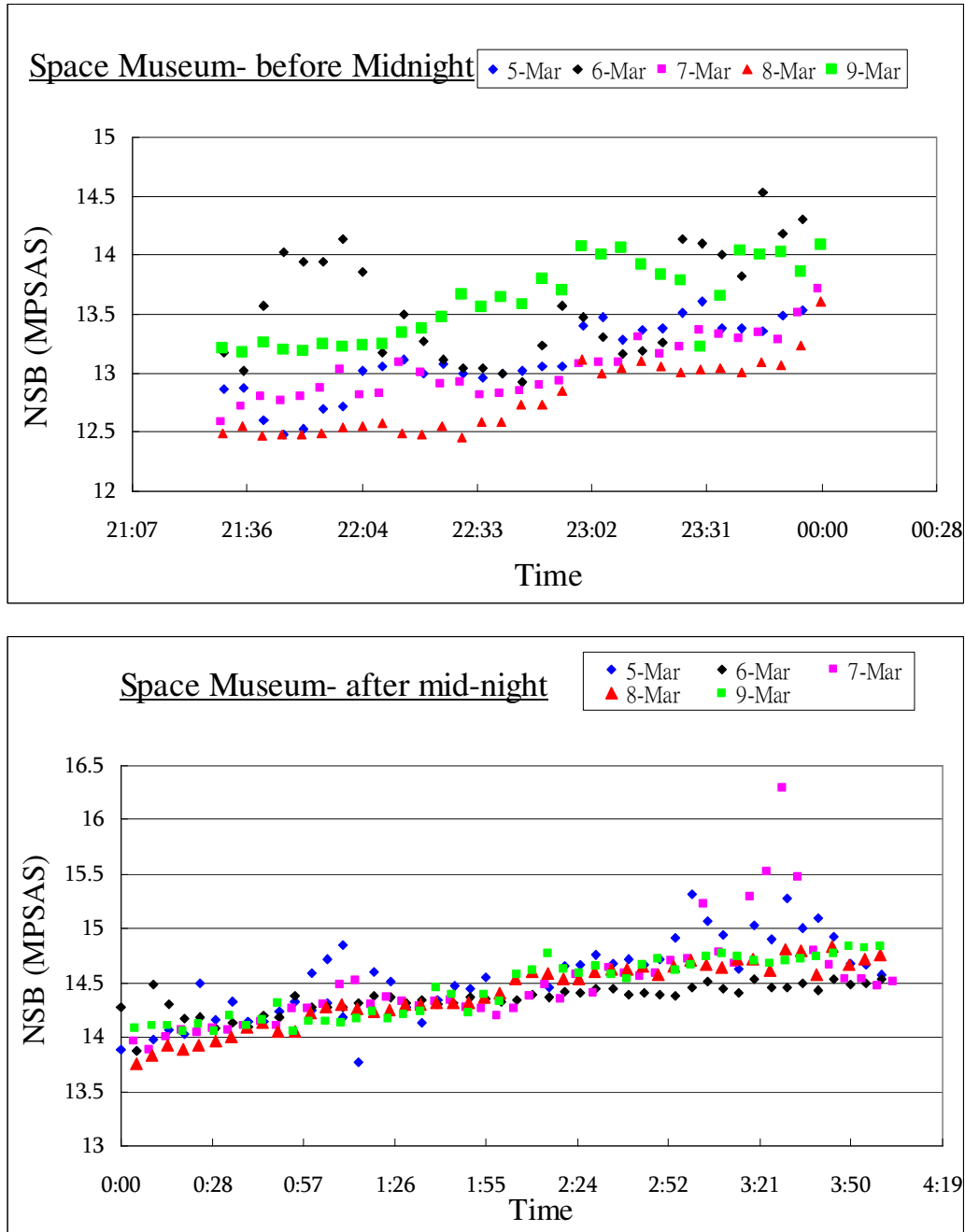


Figure 32 and 33. Graphs showing the time consistence of SQM-LE reading at Space museum

The more consistent trend after midnight can be shown by the smaller standard deviation value for the mean NSB in these periods of time.

Space Museum	Date					Standard Deviation
	5/3/09	6/3/09	7/3/09	8/3/09	9/3/09	
Average NSB Before midnight	13.11	13.57	13.04	12.79	13.61	0.3549
Average NSB After midnight	14.53	14.35	14.49	14.40	14.44	0.0712

Table 5. Comparison table for the mean NSB and the standard deviations of NSB in Figure 32 and 33.

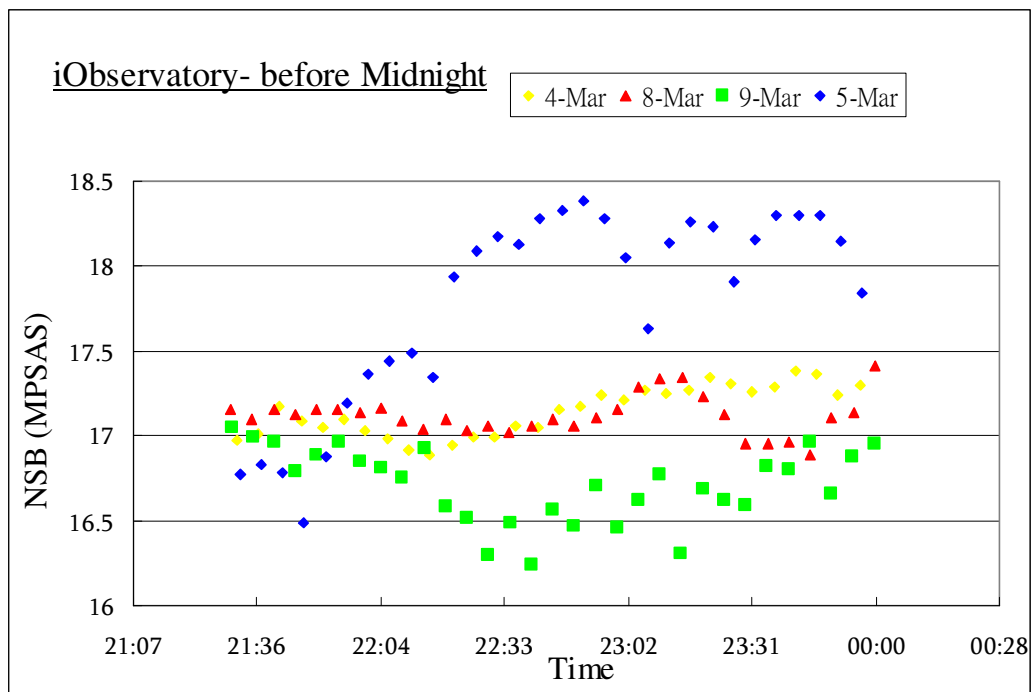


Figure 34. Graphs showing the time consistence of SQM-LE reading at iObservatory

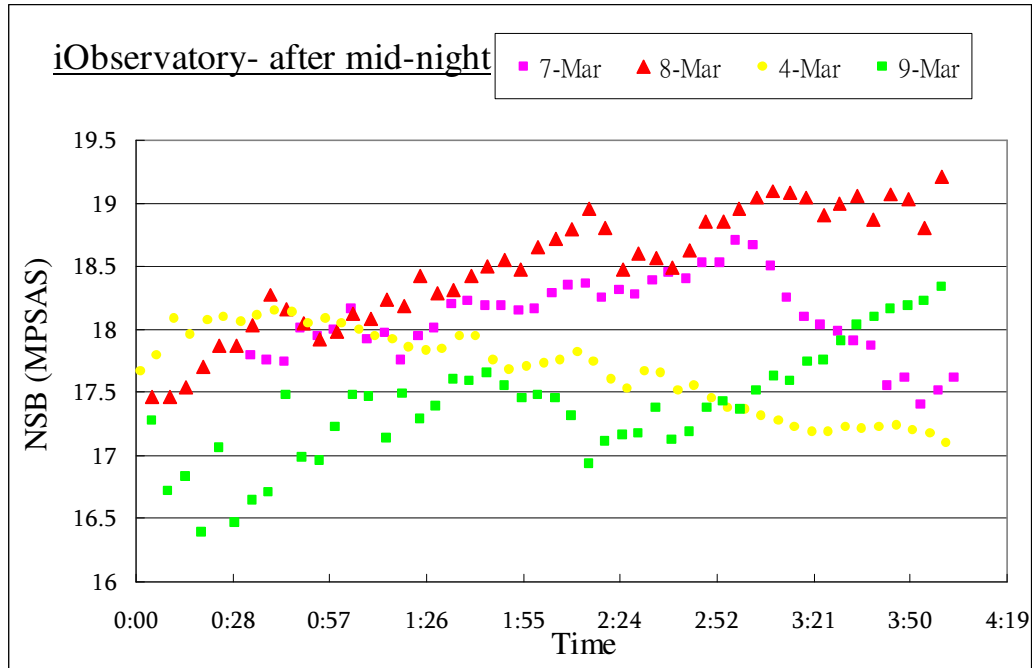


Figure 35. Graphs showing the time consistence of SQM-LE reading at iObservatory

Similarly, the statistical results are summarized in Table 6.

iObservatory	Date					Standard Deviation
	4/3/09	5/3/09	7/3/09	8/3/09	9/3/09	
Average NSB Before midnight	17.14	17.78	No data	17.12	16.71	0.44181
Average NSB After midnight	17.68	No data	18.10	18.49	17.39	0.48156

Table 6. Comparison table for the mean NSB and the standard deviations of NSB in Figure 34 and 35.

Here at iObservatory the standard deviations are similar before and after midnight. This may be due to the fact that the NSB is less affected by light pollution even late at night so that the NSB depends more on natural factors such as cloud amount and cloud base height. The possible variation brought by environmental factors is covered in the next section.

3.2.4 Abnormal peaks and discontinuities

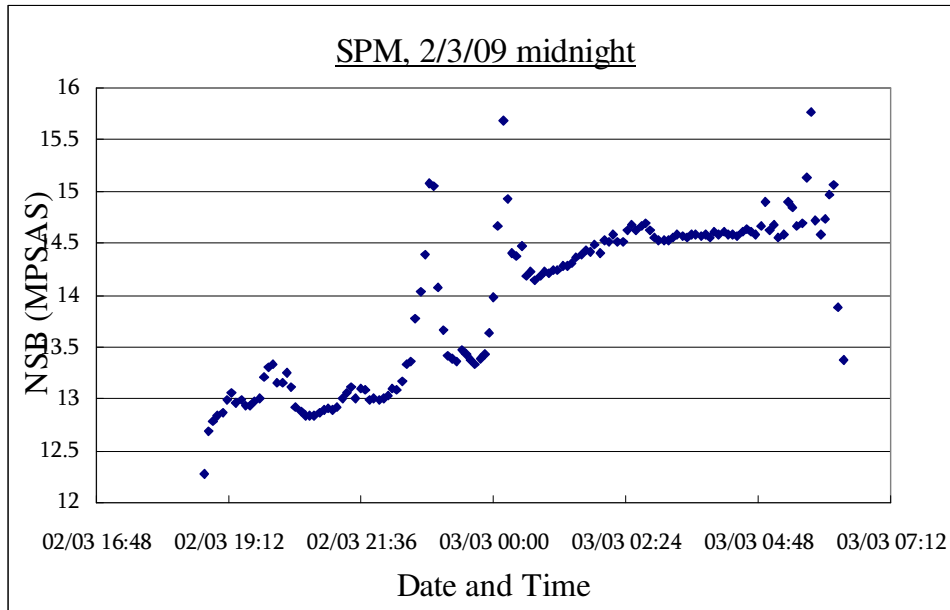


Figure 36. Two peaks found from the SQM-LE data.

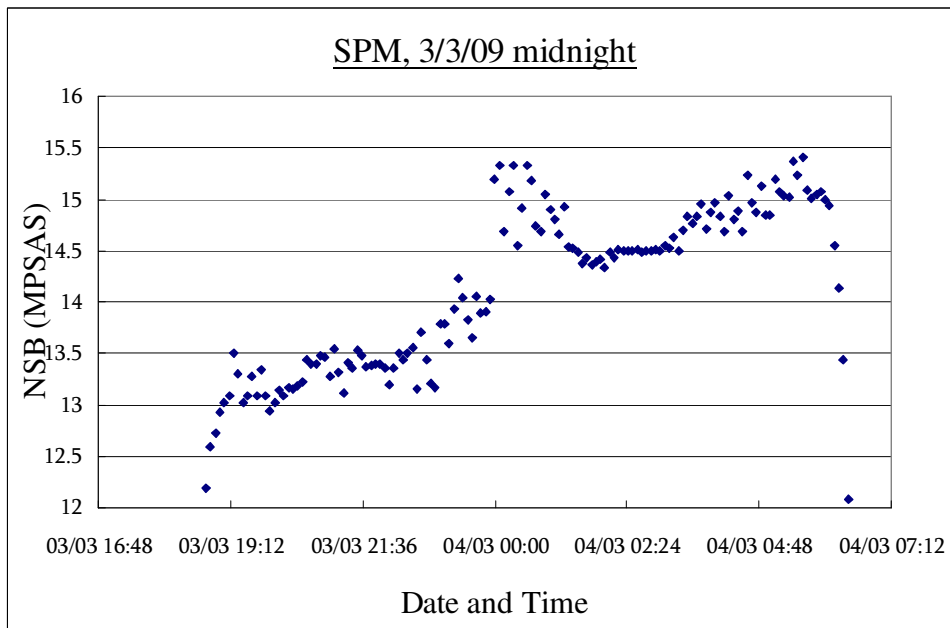


Figure 37. A sudden jump in NSB found from SQM-LE data

On the above graphs peaks and discontinuity of various scales are observed. It is believed that those all caused by the rapid change of atmospheric conditions such as cloud shifting. However, no conclusion could be made at this stage as no other information is available for deduction at this stage.

3.3 All-sky camera data analysis

3.3.1 Targeted field

The night sky in the observation night was recreated by the software SkyChart III³³ Demo version. It was chosen for its plain and simple display so that the stars in targeted field can be shown clearly below; the more interactive Stellarium³⁴ was used for quick search.

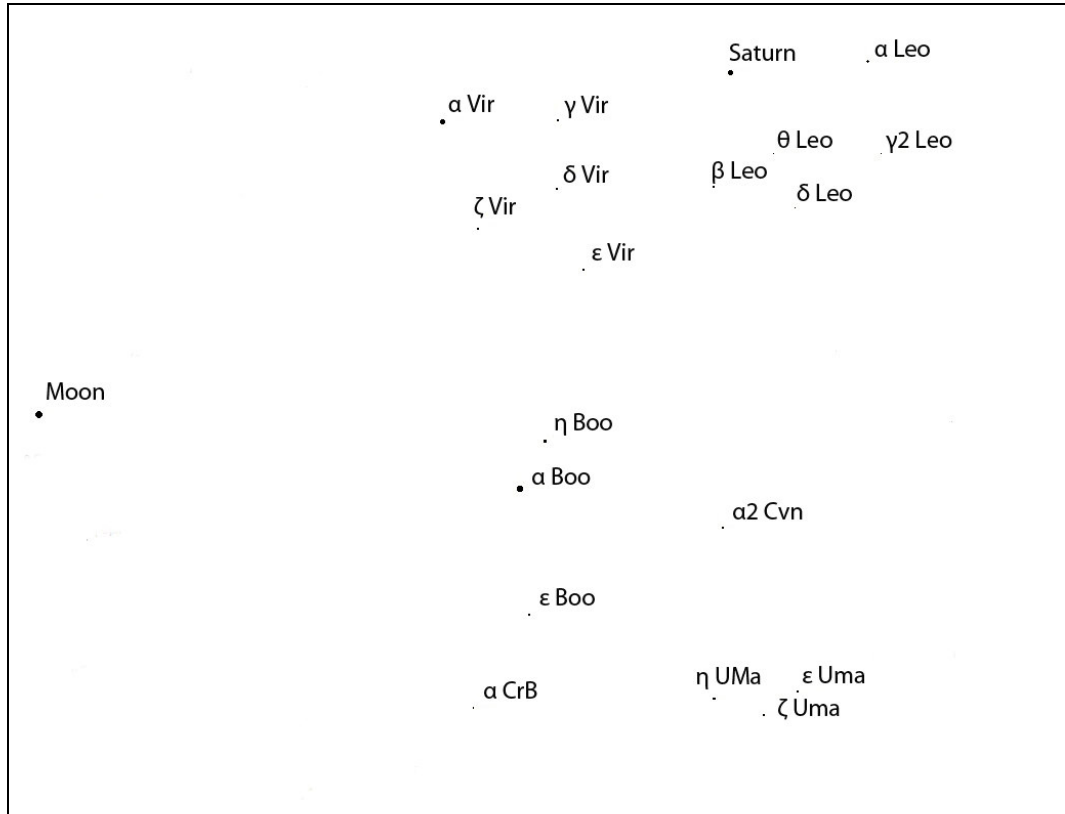


Figure 38. Targeted field of the all-sky camera

Extra attention should be paid to the vertical inversion of the image on CCD caused by the optical elements of the lens. After entering the correct location of Hong Kong, date and time of observation, Figure 38 was obtained by further choosing 'mirror-image vertically' under the 'field' option of the 'View' menu. There were many other stars originally shown in Figure 38 but they were masked for their not showing on the data frames.

3.3.2 Plate scale estimation

From the targeted field generated by the SkyChart III, the stars in the data frames were identified. It is observed that the image fields were not distorted very much by the fisheye lens. The shape of positions of the stars stays roughly the same in all the

data frames. To calculate the sky brightness using equation (10) and (12), the angular field of view and thus the plate scales should be determined first. As described in the methodology section 2.6.4, the plate scales are found by relating the pixel distance with the angular distance between two reference stars. 5 pairs of stars were chosen for a 60-second exposure image frame, Figure 39.



Figure 39. Five regions chosen to determine the plate scales

The RA and Dec of the stars in the frame were obtained from the SIMBAD database and the results are tabulated with the x and y pixel values.

	RA (in hour)				Dec (in degree)					
	Hou r	Minut e	Secon d	Decima l	Degre e	Arcmi n	Arcse c	Decima l	Pixel X	Pixel Y
α Vir	13	25	40.79	13.428	-11	-12	-32.6	-11.209	1265	2040
γ Vir	12	42	7.97	12.702	-1	-29	-59.4	-1.500	1717	2100
δ Vir	12	56	4.35	12.935	3	20	51.7	3.348	1749	1924
ϵ Vir	13	2	38.28	13.044	10	54	35.1	10.910	1885	1728
ζ Vir	13	35	9.96	13.586	0	38	34.3	0.643	1453	1776
α Boo	14	16	5.61	14.268	19	8	23.6	19.140	1717	1144
η Boo	13	55	7.42	13.919	18	21	9.9	18.353	1797	1284
ϵ Boo	14	45	23.38	14.756	27	2	8.7	27.036	1801	836

α Leo	10	8	51.84	10.148	11	55	18.7	11.922	2905	2492
β Leo	11	49	32.04	11.826	14	31	15	14.521	2361	2020
θ Leo	11	14	43.38	11.245	15	22	45.5	15.379	2581	2152
δ Leo	11	14	35.73	11.243	20	28	24.4	20.473	2681	2024
γ^2 Leo	10	20	28.82	10.341	19	47	38.9	19.794	2985	2236
α CrB	15	35	4.61	15.585	26	41	3.7	26.684	1617	552
η UMa	13	47	54.27	13.798	49	16	3.5	49.268	2561	720
ζ UMa	13	24	17.57	13.405	54	52	39.1	54.878	2761	696
ϵ UMa	12	54	25.8	12.907	55	54	36.1	55.910	2877	772
α^2 CVn	12	56	27.62	12.941	38	16	7.2	38.269	2513	1160

Table 7. Position values for the stars visible in the data frame

2

The plate scale can then be estimated by dividing the angular distance by the pixel distance. The results of the 5 pairs chosen are tabulated below.

Region	Star pairs		Distance (degree)	Distance (arcsec)	Distance (pixel)	Plate Scale (arcsec/pixel)
1	α Boo	η Boo	5.026	18094.10	161.25	112.2148
2	θ Leo	δ Leo	5.094	18339.22	162.43	112.9043
3	ζ UMa	ϵ UMa	4.362	15701.56	138.68	113.2219
4	α Leo	γ^2 Leo	8.352	30068.37	268.21	112.108
5	γ Vir	δ Vir	5.969	21489.55	178.89	120.1302

Table 8. Plate scale estimation

It is deduced that the plate scale values do not have explicit dependence on the image position. The plate scale is around 110 arcsec per pixel.

3.3.3 Sky brightness estimation

Due to the insensitive dependence of the plate scale on the position in the frame, the angular field of view F of equation (13) is assumed to be constantly 110 arcsec/pixel across the frames. The sky brightness values estimated by the method

discussed in section 2.6.4 on 4 different data frames are shown in Table 5 and 6.

Frames	Reference Star	Flux	Position X	Position Y	Peak
001emp3ds	α Boo	4.00E+06	1683.81	1097.79	16703
	α Vir	7.63E+05	1220.42	1992.14	5216
001emp6ds	α Boo	7.97E+06	1719.73	1145.61	29319
	α Vir	1.53E+06	1262.97	2040.4	9902
002emp3ds	α Boo	4.00E+06	1688.19	1103.97	17059
	α Vir	7.89E+05	1225.47	1998.48	5531
003emp3ds	α Boo	3.11E+06	1937.54	1411.63	11279
	α Vir	5.51E+05	1516.54	2312.02	4289
003emp6ds	α Boo	1.39E+06	1978.31	1456.89	3891
004emp3ds	α Boo	2.28E+06	1942.69	1417.35	8264
004emp6ds	α Boo	2.30E+06	1985.62	1464.95	7882

Table 9. Result table for flux estimation of reference stars

Frames	Section	Median	Stdev	Actual Flux	Plate Scale					
					110 arcsec/ pixel			120 arcsec/pixel		
					Flux/FOV	Reference stars		Flux/FOV	Reference stars	
						α Boo	α Vir		α Boo	α Vir
						MPSAS	MPSAS		MPSAS	MPSAS
001emp3ds	1	2507	60.1	4211.76	0.348	18.17	17.40	0.292	18.36	17.58
2:11:54	2	2073	66.2	3482.64	0.288	18.38	17.60	0.242	18.57	17.79
	3	2659	77.1	4467.12	0.369	18.11	17.33	0.310	18.30	17.52
					Average	18.22	17.44	Average	18.41	17.63
	SQM reading		19.1		Difference	0.88	1.66	Difference	0.69	1.47
001emp6ds	1	5425	156	9114.00	0.753	18.08	17.31	0.633	18.27	17.50
2:20:22	2	3617	83.1	6076.56	0.502	18.52	17.75	0.422	18.71	17.94
	3	5432	106	9125.76	0.754	18.08	17.31	0.634	18.27	17.50
					Average	18.23	17.46	Average	18.42	17.64
	SQM reading		19		Difference	0.77	1.54	Difference	0.58	1.36
002emp3	1	2633	90.1	4423.44	0.366	18.12	17.38	0.307	18.31	17.57
2:12:56	2	2523	79.2	4238.64	0.350	18.17	17.43	0.294	18.36	17.61
	3	2726	54.4	4579.68	0.378	18.08	17.34	0.318	18.27	17.53
					Average	18.12	17.38	Average	18.31	17.57
	SQM reading		19.1		Difference	0.98	1.72	Difference	0.79	1.53
003emp3	1	3798	108	6380.64	0.527	17.45	16.59	0.443	17.64	16.78
3:07:05	2	3446	60.4	5789.28	0.478	17.55	16.70	0.402	17.74	16.89
	3	2315	56.1	3889.20	0.321	17.99	17.13	0.270	18.18	17.32
	4	2171	58.8	3647.28	0.301	18.06	17.20	0.253	18.25	17.39
					Average	17.69	16.83	Average	17.88	17.02
	SQM reading		19		Difference	1.31	2.17	Difference	1.12	1.98

Table 10. Result table for sky brightness estimation. NSB is in MPSAS and plate scale is in arcsecond/pixel.

From Table 10, all the estimated values of sky brightness are less than the corresponding SQM values. This means the prediction made by the all-sky camera yields a brighter value than reality.

In equation (10), the magnitudes of the reference stars found in the SIMBAD database are obtained by applying filters of various bands. However, the data frames taken by the all-sky camera did not adopt any filter so all wavelengths were allowed to reach the CCD. As a result, wavelength outside V-band could also contribute to certain count on each pixel thus overestimating the flux of the reference stars, giving rise to a brighter sky estimated.

The change of magnitude at the zenith brought by the moon is calculated to be about -2.5 MPSAS on that night, by the program discussed in section 2.4. The deviation of the estimated sky brightness from the SQM reading was the largest in the last data frame since the moon is completely inside the image. The selection of image sections to estimate the sky background would then affect the final sky brightness value calculated quite a lot.

Another observation made is that the sky brightness values estimated by different reference stars are consistently different, with α Vir producing a brighter sky. The α Boo and α Vir are of spectral type K and B respectively. α Vir will generally emit light of longer wavelengths than α Boo. The quantum efficiency of the CCD plate is not constant throughout the spectrum. From Figure 13 the CCD used in the present study is more sensitive at the red end, so the flux of α Vir would be underestimated. By equation (11) a smaller f_{star} would in turn induce a smaller sky magnitude, as calculated in Table 10 for α Vir.

The result suggests that the photometric study of sky brightness by the all-sky camera image is possible but the sources of error should be minimized and taken into account. The presence of error in different part of the study will be discussed in section 4.

4. Sources of error and improvements

4.1 Reliability of SQM readings

In section 3.1, data were collected by different people at different places. Random error introduced by the involvement of manpower must be taken into account in the analysis of data. The observation sites are close to where participants live so the contribution of artificial light to the readings is also not to be underestimated. Extra care should be taken for science research involving huge amount of manpower as uncertainties are inevitably brought along with the reliance on human.

4.2 Casing of SQM-LE

A simple plastic case was used to accommodate the SQM-LE in this preliminary model. The wearing of the case by outdoor environment would blur the window opened for NSB detection so that more scattering would be caused by the case. Dust or raindrops dissipated on the casing top would also contribute to unwanted scattering.

Removable transparent hemispherical cover can be used as the detection window to avoid accumulation and to facilitate the drying of water.

4.3 All-sky camera images

There are a number of errors included in the determination of sky brightness using the all-sky camera images. The inevitable one is the natural Poisson noise arose from the image taking process which comes along with all kind of natural phenomena. By subtracting the image frames by the master dark frames, additional noise would be introduced although more dark frames could be taken to minimize that.

Light took different paths to reach the CCD from the fisheye lens. It would be attenuated by different extent with different optical path due to defects in optics and misalignment of components. This systematical variation can be corrected by flat fielding, that is dividing the data frames by a master flat frame combined from few images of evenly illuminated surface.

Atmospheric conditions and light pollution did also affect the sky brightness estimation. As in all the data frames taken, the top parts of the images were brightened by the light from the Sai Kung town direction. The presence of the moon did brighten up all the data frames which were not calculated. In typical photometry, various filters are used to obtain data for the colour transformation equation so that the instrumental values of the system can be converted into the standard one.

5. Acknowledgement

I would like to take this opportunity to express my heartfelt gratitude to Dr. Pun for his patience, guidance and professional suggestions given throughout the whole project. Also, the project would not be going so well without Mr. So Chu Wing's support and advice. It was a great experience to be involved in this project and I look forward to the presentation to be held weeks later.

6. Appendix

6.1 C++ program script for the moon phase/ position calculation

```
#include <fstream>
#include <iostream>
#include <math.h>
#include <iomanip>
using namespace std;

double pi=3.14159265358979;
double rad=pi/180.0;
double deg=180.0/pi;
double epcilon=23.43333333;           //the obliquity of the ecliptic
double lon=114.16666667;             //Geometric longitude in degree,
positive east
double lat=22.3;                     //Geometric latitude in degree, positive north

//To calculate the day number from 2000 Jan 0.0 (input with Hong Kong Local
Time, 24-hour clock)
double daynumber(int year, int month, int date, int hour, int min, int
sec)
{
double dwhole; double dfrac; double jd;

//Convert Hong Kong Local Time to decimal UT
hour-=8;    //since Hong kong's time zone GMT=+8
if (hour<0) {hour+=24; date-=1;} // "hour" would not be greater than 24
//Compute the fraction of day
dfrac = (double)(hour + min/60.0 + sec/3600.0)/24.0;
//Compute number of whole day
dwhole
=(double)367*year-int(7*(year+int((month+9)/12))/4)+int(275*month/9)+
date-730530.0;
jd=dwhole+dfrac; //Add up to obtain the day number
return jd;
}

//=====
```

```

//Function to lie an angle between 0 and 360
double Range(double x)
{
if (x>0 && x<360) {return x;}
else
{
if (x<0) {while (x<0) x+=360;}
else {while (x>360) x-=360;}
return x;
}
}
//=====

//Function displaying decimal form as hours/degree form
void Hd(double d)
{
int hour; int min; int sec;
hour=int(d);
min=int((d-int(d))*60);
sec=int((((d-int(d))*60)-int(((d-int(d))*60)))*60);
cout<<hour<<": " <<min<<": " <<sec<<"\n";
}
//=====

//To adjust to the correct quadrant after taking arctangent
double qua(double x, double y)
{
double w=atan(y/x)*deg;
if (x==0) {if (y>0) {w=90;} if (y<0) {w=-90;} }
if (x<0 && y<0) {w+=180;} //adjust to the
correct quadrant as x and y
if (x<0 && y>0) {w+=180;}
if (x>0 && y<0) {w+=360;}
return w;
}
//=====

```

```

//To calculate the Sun's ecliptic longitude
double Sun(int year, int month, int date, int hour, int min, int sec, int
i)
//value of "i" controls the return value
{
double w=282.9404+4.70935E-05*daynumber(year, month, date, hour, min,
sec);          //Longitude of perigee
double a=1.000000;

//Mean distance from the earth, in AU
double e=0.016709-1.151E-09*daynumber(year, month, date, hour, min,
sec);
//Eccentricity
double M=356.0470+0.9856002585*daynumber(year, month, date, hour, min,
sec);          //Mean anomaly
double obliquity=23.4393-3.563E-07*daynumber(year, month, date, hour,
min, sec);      //Obliquity of the ecliptic

double L=w+M;          //The sun's mean longitude
double E=M+deg*e*sin(M*rad)*(1+e*cos(M*rad));

//compute the sun's rectangular coordinates on the plane of ecliptic
(x-axis points to perigee)
double x=cos(E*rad)-e;
double y=sin(E*rad)*sqrt(1-e*e);
    //convert to ecliptic longitude
double v=qua(x,y);
//double v=atan(y/x);    //True anomaly
//if (v<0) {v+=pi;}
double longitude=v+w;

if (i==0) {return Range(longitude);}    //in decimal hour
if (i==1) {return Range(L);}    //return sun's mean longitude, for later
calculations
if (i==2) {return Range(M);}    //return sun's mean anomaly, for later
calculations
}
//=====

```



```

//To convert ecliptic coordinate to RA and Dec (input with degrees)
double Equatorial(double lamda, double beta, int i)
{
//calculation of right ascension
double
alpha=atan(tan(lamda*rad)*cos(epsilon*rad)-tan(beta*rad)*sin(epsilon*
rad)/cos(lamda*rad)); //result is in radian

if (alpha>0)
{
if (lamda>180 && lamda <360) // correction
{alpha+=pi;}
}

if (alpha<0) // correction
{
if (lamda<360 && lamda>180) {alpha+=2*pi;}
if (lamda>0 && lamda<180) {alpha+=pi;}
}

//calculation of declination
double
delta=asin(sin(beta*rad)*cos(epsilon*rad)+cos(beta*rad)*sin(epsilon*r
ad)*sin(lamda*rad)); //result is in radian

//outputting the RA and DEC
if (i==0) { return (alpha*deg/15);} //RA output in hour
if (i==1) {return (delta*deg);} //Dec output in degree
}
//=====

```

```

//To calculate the Local Sideral Time (it is counted from the vernal equinox,
i.e. a fixed point in space-->>RA(in hour)=LST to transit-->>LST count
00:00 from
//overlapping of SOUTH and vernal equinox, then celestial sphere turns
around, stars meets the SOUTH

double LST(int year, int month, int date, int hour, int min, int sec) //this
requires input as local time, UT will be generated automatically in program
{
double lst; double ut;
double w=282.9404+4.70935E-05*daynumber(year, month, date, hour, min,
sec);

//Longitude of perigee in degree
double M=356.0470+0.9856002585*daynumber(year, month, date, hour, min,
sec);          //Mean anomaly in degree
double L=w+M;
//The sun's mean longitude in degree

L+=180.0;
L=Range(L);

hour-=8;      //Hong kong's time zone GMT=+8, changing to UT
if (hour<0) {hour+=24; date-=1;} //"hour" would be positive, not being
greater than 24;
ut=hour+min/60.0+sec/3600.0;    //in decimal hour
//parts of day is should NOT be added until here
ut*=15;          //to decimal degree
lst=Range(L+ut+lon)/15;        //back to decimal hour
return lst;      //in decimal hour
}

```

```

void main()
{
int year; int month; int date; int hour; int min; int sec;
int dates;
ifstream file_in("Database_DT.txt"); //read from file_date.txt, input
to program
ofstream file_out("file_80.txt"); //Write results to file_moon.txt, from
program

cout<<"How many date(s) are there?";cin>>dates;

for (int k=0; k<dates; k++)
{
    file_in>>year>>month>>date>>hour>>min>>sec;
double N=125.1228- 0.0529538083* daynumber(year, month, date, hour, min,
sec);          //Longitude of the ascending node, in degree
double i = 5.1454;
//Inclination of the lunar orbit realtive to the ecliptic, in degree
double w=318.0634+ 0.1643573223* daynumber(year, month, date, hour, min,
sec);          //Argument of perigee, in degree
double a = 60.2666;
//Mean distance from the earth, in earth equatorial radii
double e = 0.054900;
//Eccentricity of orbit
double M = 115.3654+ 13.0649929509* daynumber(year, month, date, hour,
min, sec);          //Mean anomaly, in degree
N=Range(N);
w=Range(w);
M=Range(M);

//After obtaining those orbital elements, we compute the eccentric anomaly
E
double E0=M+deg*e*sin(M*rad)*(1+e*cos(M*rad)); //First approximation,
E0 is in degree
double E1=E0-((E0-deg*e*sin(E0*rad)-M)/(1-e*cos(E0*rad)));
//Iteration formula to reduce the error
while (abs(E1-E0)>1E-05) //Setting the error bound for the first
                        calculation, also in degree

```

```

{
    E0=E1;                                     //Put E1 to be our new E0
    E1=E0-((E0-deg*e*sin(E0*rad)-M)/(1-e*cos(E0*rad)));
    //Calculate new E1
}

double E=E1;    //This E1 will be our Eccentric anomaly E after iteration,
in degree again

//Moon's distance and true anomaly
double x = a * (cos(E*rad) - e); //rectangular coordinates in plane of
lunar orbit, centred on earth (focus)
double y = a * sqrt(1 -e*e)*sin(E*rad);

//converting to distance and true anomaly
double r=sqrt(x*x+y*y);           //geocentric distance
double v=qua(x,y);               //true anomaly

//converting to the ecliptic coordinates (rectangular)
double xeclip = r * ( cos(N*rad) * cos((v+w)*rad) - sin(N*rad) *
sin((v+w)*rad) * cos(i*rad));
double yeclip = r * ( sin(N*rad) * cos((v+w)*rad) + cos(N*rad) *
sin((v+w)*rad) * cos(i*rad));
double zeclip = r *sin((v+w)*rad) * sin(i*rad);
double reclip=sqrt(xeclip*xeclip+yeclip*yeclip+zeclip*zeclip);
//lunar distance

//converting to ecliptic longitude, latitude and distance
double elon=qua(xeclip, yeclip);           //in degree
double elat=asin(zeclip/reclip)*deg;       //in degree

//Perturbations by the sun
double Ls=Sun(year, month, date, hour, min, sec, 1); //Sun's mean
longitude
double Lm=Range(N+w+M); //Moon's mean longitude, for the moon
double Ms=Sun(year, month, date, hour, min, sec, 2); //Sun's mean
anomaly
double Mm=M;                               //Moon's mean anomaly:
double D=Lm- Ls;                           //Moon's mean elongation:

```

```

double F=Lm- N;                                //Moon's argument of latitude

//convert to radian for computations
Ls*=rad; Lm*=rad; Ms*=rad; Mm*=rad; D*=rad; F*=rad;

//Perturbations in longitude, results are all in degree
double perlon=(-1.274* sin(Mm - 2*D))+(+0.658* sin(2*D))+(-0.186*
sin(Ms))+(-0.059* sin(2*Mm - 2*D))+(-0.057* sin(Mm - 2*D + Ms))+(+0.053*
sin(Mm + 2*D));
perlon+=(+0.046* sin(2*D - Ms))+(+0.041* sin(Mm - Ms))+(-0.035*
sin(D))+(-0.031* sin(Mm + Ms))+(-0.015* sin(2*F - 2*D))+(+0.011* sin(Mm
- 4*D));

//Perturbations in latitude
double perlat=(-0.173* sin(F - 2*D))+(-0.055* sin(Mm - F - 2*D))+(-0.046*
sin(Mm + F - 2*D))+(+0.033* sin(F + 2*D))+(+0.017* sin(2*Mm + F));

//Perturbations in lunar distance
double perdis=(-0.58 * cos(Mm - 2*D))+(-0.46 * cos(2*D));

//Adding the perturbations
elon+=perlon;                                //ecliptic longitude of the moon, degree
elat+=perlat;                                //ecliptic latitude of the moon, degree
reclip+=perdis;                              //lunar distance

//Obtain the RA and Dec
double RA=Equatorial(elon, elat, 0)*15;      //moon's RA in decimal
degree
double Dec=Equatorial(elon, elat, 1);        //moon's Dec in degree
double HA=Range(15*LST(year, month, date, hour, min, sec)-RA); //in
degree

//Converting to rectangular coordinates, x-axis points in celestial
sphere's South
double X = cos(HA*rad)* cos(Dec*rad);
double Y = sin(HA*rad)* cos(Dec*rad);
double Z = sin(Dec*rad);

```

```

//Rotate above system along y-axis by (90-latitude) degree
double xhor = X * sin(lat*rad) - Z * cos(lat*rad);
double yhor = Y;
double zhor = X * cos(lat*rad) + Z * sin(lat*rad);

double azimuth=Range(qua(xhor,yhor)+180);
double altitude=asin(zhor)*deg;
//Phase of the moon
double d=180-Sun(year, month, date, hour, min, sec, 0)+elon;
double Phase=0.5*(1+cos(d*rad));

//Moon's distance
if (altitude>80) {file_out<<"Yes";}
else {file_out<<"No";}
file_out<<"\n";

//write the answer to file_output.txt
//file_out<<year<<" "<<month<<" "<<date<<" "<<hour<<" "<<min<<"
"<<sec<<" "<<azimuth<<" "<<altitude<<" "<<Phase<<"\n"; //output the
results
}
cout<<"Done!"<<"\n";
cout<<"Please find the results in the file 'file_output.txt'.";
}

```

6.2 C++ program script for the change in magnitude calculation

```
#include <fstream>
#include <iostream>
#include <math.h>
#include <iomanip>
using namespace std;

double pi=3.14159265358979;
double rad=pi/180.0;
double deg=180.0/pi;
double epsilon=23.43333333;           //the obliquity of the
ecliptic (23deg 26')
double lon=114.16666667;              //(114deg 10')
Geometric longitude in degree, positive east
double lat=22.3;                      // (22deg 18')
Geometric latitude in degree, positive north
double k=0.172;                       //value of extinction coefficient

void main()
{
double dates;
ifstream file_in("Data_theory_altitude.txt"); //read from
file_date.txt, input to program
ofstream file_out("42_file_Theory_alt_dV_1.txt"); //Write results to
file_moon.txt, from program

cout<<"How many date(s) are there?";cin>>dates;

for (int k=0; k<dates; k++)
{
double altitude;
double d=0; //new moon means 180; full moon means zero; quater means
90
file_in>>altitude;

if (d>360) {d-=360;}
if (d>180) {d=d-360;}
```

```

double Phase=0.5*(1+cos(d*rad));

// Adding the brightness part
//double Airmass(double Z)//airmass, input degree

double Zs=0; //zenith distance of the sky position
double Zm=90-altitude; //zenith distance of the moon
double XZs=pow(1-0.96*pow(sin(Zs*rad),2),-0.5); //Scattering
airmass, value of X
double XZm=pow(1-0.96*pow(sin(Zm*rad),2),-0.5); //return XZ;

//double Illumin(double alpha) //Illuminance of the moon, input
degree(phase angle)
double I=pow(10,-0.4*(3.84+0.026*fabs(d)+4*pow(10,-9)*pow(d,4)));
//return I;

//double scafunc(double rho) //Scattering function, input angular
distance between sky and the moon in degree
double rho=0;
double
fp=pow(10,5.36)*(1.06*pow(cos(rho*rad),2))+pow(10,6.15-rho/40);
//return fp;

//double moonbright(double rho, double alpha, double Zm, double Z)
double Bmoon=fp*I*pow(10,-0.4*0.172*XZm)*(1-pow(10,-0.4*0.172*XZs));
//double
B=scafunc(rho)*Illumin(alpha)*pow(10,-0.4*k*Airmass(Zm))*(1-pow(10,-0
.4*k*Airmass(Z)));
//return B;
//double Bnought(double Z) //dark night time sky brightness

double Bzen=79.0;
double B0=Bzen*pow( 10,-0.4*k*(XZs-1)*XZs );
//return B0;
double dV=-2.5*log10((Bmoon+B0)/B0);
//return dV;
file_out<<dV<<"\n";
}

```


7. Reference:

1. Woodside M. Thomas Edison: The man who lit up the world. Sterling; 2007. 124p.
2. Longcore T, Catherine R. Ecological light pollution. *Frontiers in Ecology and the Environment* 2004.
3. Chepesiuk R. Missing the dark: health effects of light pollution. *Environ Health Perspect* 2009; 117(1): A20-A27.
4. Facebook webpage 'Save the Night'
<http://www.facebook.com/group.php?gid=28797635928>
5. My Space webpage 'Turndownthelight'
<http://www.myspace.com/turndownthelight>
6. Jensen H. W. A physically-based night sky model. *International Conference on Computer Graphics and Interactive Techniques* 2001. p399-408.
7. Duriscoe D. M, Luginbuhl C. B, Morre C. A. Measuring night-sky brightness with a wide-field CCD camera 2007. 119: 192-213.
8. Sanchez S. F, Aceituno J, Thiele U, Perez-Ramirez D, Alves J. The night sky at the Calar Alto observatory 2007. 119: 1186-1200.
9. Dark skies awareness: an IYA2009 cornerstone project.
<http://www.darkskiesawareness.org/>
10. A survey of light pollution in Hong Kong:
<http://nightsky.physics.hku.hk/index.asp>
11. Unihedron's SQM webpage: <http://unihedron.com/projects/darksky/>
12. Cinzano P. Night sky photometry with sky quality meter. ISTIL internal report 2005.
13. Google Earth webpage: <http://earth.google.com/>
14. SQM-LE user manual:
http://unihedron.com/projects/sqm-le/cd/SQM-LE_Users_manual.pdf
15. D-Link official webpage for DWL-P200:
<http://www.dlink.com/products/?sec=1&pid=332>
16. SQM Reader webpage at Knightware: <http://www.knightware.biz/sqm/reader.htm>
17. Bradley E. Schaefer: Telescopic limiting Magnitudes (1990) Pub. ASP 102:212-229
18. photo
19. Computing planetary positions: <http://www.stjarnhimlen.se/comp/tutorial.html>
20. Seismology, time and astronomy, Hong Kong Observatory:
http://www.hko.gov.hk/gts/event/event-solar-eclips1_e.htm?menu=events&addbar
21. Krisciunas K. A model of the brightness of moonlight. *Publications of the*

- astronomical society of the Pacific 1991. 103: 1033-1039
22. Environmental Protection Department webpage:
<http://www.epd-asg.gov.hk/english/pastapi/pastapie.php>
 23. Nikon official webpage:
<http://www.nikon.com.hk/productitem.php?pid=94-272a3f1aad>
 24. Photo equipment: <http://goeringlaw.com/Photo%20Equipment.html>
 25. SBIG STL-11000M:
<http://www.allaboutastro.com/equipmentpages/sbig11000.html>
 26. STL catalog: http://www.sbig.com/pdf/files/STL_catalog2.pdf
 27. IRAF project homepage: <http://iraf.noao.edu/>
 28. SAOImage DS9: <http://hea-www.harvard.edu/RD/ds9/>
 29. imexamine help page: <http://stdas.stsci.edu/cgi-bin/gethelp.cgi>
 30. Romanishin W. An Introduction to Astronomical Photometry Using CCDs. 2002.
 31. SIMBAD main page: <http://simbad.u-strasbg.fr/simbad/>
 32. Calculation of angle between stars:
<http://users.zoominternet.net/~matto/Java/Angle%20between%20two%20stars.htm>
 33. SkyChart III webpage: <http://www.southernstars.com/skychart/index.html>
 34. Stellerium webpage: <http://www.stellarium.org/>